



Can high-resolution GCMs reach the level of information provided by 12-50 km CORDEX RCMs in terms of daily precipitation distribution?

Marie-Estelle Demory¹, Ségolène Berthou², Silje L. Sørland¹, Malcolm J. Roberts², Urs Beyerle¹, Jon Seddon², Rein Haarsma³, Christoph Schär¹, Ole B. Christensen⁴, Rowan Fealy⁵, Jesus Fernandez⁶, Grigory Nikulin⁷, Daniele Peano⁸, Dian Putrasahan⁹, Christopher D. Roberts¹⁰, Christian Steger¹¹, Claas Teichmann¹², Robert Vautard¹³

¹ Institute for Atmospheric and Climate Science, ETH, 8092 Zürich, Switzerland

² Met Office Hadley Centre, EX1 3PB Exeter, United Kingdom

³ KNMI, 3731 GA De Bilt, Netherlands

⁴ Danish Meteorological Institute (DMI), DK-2100 Copenhagen, Denmark

⁵ ICARUS/Department of Geography, Maynooth University, Maynooth, Co. Kildare, Ireland

⁶ University of Cantabria, 39005 Santander, Spain

⁷ Swedish Meteorological and Hydrological Institute (SMHI), SE-60176 Norrköping, Sweden

⁸ CMCC, 40127 Bologna, Italy

⁹ Max-Planck-Institut für Meteorologie (MPI), 20146 Hamburg, Germany

¹⁰ ECMWF, RG2 9AX Reading, United Kingdom

¹¹ Deutscher Wetterdienst (DWD), 63067 Offenbach, Germany

¹² Climate Service Center Germany (GERICS), Helmholtz-Zentrum Geesthacht, 20095 Hamburg, Germany

¹³ Institut Pierre-Simon Laplace, Paris, France

Correspondence to: Marie-Estelle Demory (marie-estelle.demory@env.ethz.ch)

Abstract. In this study, we perform an evaluation of PRIMAVERA high-resolution (25-50 km) Global Climate Models (GCMs) relative to CORDEX Regional Climate Models (RCMs) over Europe (12-50 km resolutions). It is the first time such assessment is performed for regional climate information using ensembles of GCMs and RCMs at similar horizontal resolutions. We perform this exercise for the distribution of daily precipitation contributions to rainfall bins over Europe under current climate conditions. Both ensembles are evaluated against high quality national gridded observations in terms of resolution and station density. We show that PRIMAVERA GCMs simulate very similar distribution to CORDEX RCMs that CMIP5 cannot because of their coarse resolutions. PRIMAVERA and CORDEX ensembles generally show similar strengths and weaknesses. They are of good quality in summer and autumn in most European regions, but tend to overestimate precipitation in winter and spring. PRIMAVERA show improvements in the latter bias by reducing mid-rain rate biases in Central and Eastern Europe. Moreover, CORDEX simulate less light rainfall than PRIMAVERA in most regions and seasons, which improves this common GCM bias. Finally, PRIMAVERA simulate less heavy precipitation than CORDEX in most regions and seasons, especially in summer. PRIMAVERA appear to be closer to observations. However, when we apply an averaged precipitation undercatch error of 20%, CORDEX become closer to these synthetic datasets.



35 Considering 50 km resolution GCM or RCM datasets over Europe results in large benefits compared to CMIP5 models for
impact studies at the regional scale. The effect of increasing resolution from 50 km to 12 km in CORDEX simulations is, in
comparison, small in most regions and seasons outside mountainous regions (due to the importance of orography) and
coastal regions (mostly depending on the resolution of the land-sea contrast). Now that GCMs are able to reach the level of
information provided by CORDEX RCMs run at similar resolutions, there is an opportunity to better coordinate GCM and
40 RCM simulations for future model intercomparison projects.

1 Introduction

Climate models are essential tools to provide information on the evolution of climate quantities, their variability and
interactions with various components of the Earth System. There have been two main streams of development in the climate
modelling community: Global Climate Models (GCMs) and Regional Climate Models (RCMs). GCMs are complex models
45 that account for interactions at the global scale between various components of the Earth System (e.g. atmosphere, ocean, sea
ice, vegetation). They are designed to balance model resolution, physics complexity and computational requirements, and are
therefore commonly run at coarse spatial resolution. RCMs are complex models that dynamically downscale GCM results to
obtain fine climate information at the regional scale. The main advantages of the dynamical downscaling approach are that:
1) RCMs are computationally cheaper and use a higher horizontal resolution than state-of-the-art GCMs over the region of
50 interest. As a result, RCMs provide a more detailed representation of complex topography and land-sea contrast (e.g. Torma
et al., 2015). 2) Physical processes are based on parameterization schemes that are developed at the resolutions of the RCM
(12-50 km). At such resolution, these may be more appropriate than GCM schemes that are developed at much coarser
resolutions (100-300 km) (e.g. Giorgi and Mearns, 1999; Prein et al., 2016; Sørland et al., 2018). 3) RCMs' parameterization
schemes are specifically tuned to simulate the regional climate as realistically as possible compared to observations (e.g.
55 Bellprat et al., 2016), while it is not possible to apply regional-specific tuning in GCMs (Mauritsen et al., 2012; Hourdin et
al., 2017). 4) Each RCM can downscale various GCMs to simulate many different large-scale climate conditions at the
domain boundaries. This ability to be used in large ensembles is an important step to evaluate the RCM ensemble spread and
better constrain the model uncertainties. To provide reliable information on climate mean, variability and change to end
users at the regional to local scales, RCMs are therefore considered to be useful tools to supplement the so-called global
60 Earth System Models (such as those used for the Coupled Model Intercomparison Projects, CMIP5 and CMIP6), which are
more complex and use lower resolutions.

Since the end of the 1980s, dynamical downscaling has been used to provide regional climate projections (Dickinson et al.,
1989; Giorgi, 2019), and has become a well-accepted and extensively used approach to produce climate change information
65 at the local scale (refer to various national climate assessment reports, e.g. Kjellström et al., 2016; Fealy et al., 2018;
Fernandez et al. 2019; Sørland et al. in prep; Nationaler Klimareport



(<https://www.dwd.de/DE/leistungen/nationalerklimateport/report.html>); ReKliEs-De (<http://reklies.hlnug.de>); UK Climate Projections (<https://www.metoffice.gov.uk/research/approach/collaboration/ukcp/index>). The Coordinated Regional Climate Downscaling Experiment (CORDEX) is an international coordinated effort to produce multi-model regional climate change scenarios (Giorgi et al., 2009; Gutowski et al., 2016). CORDEX started in 2009 with the main goals to develop a framework that provides consistent high-resolution climate information at the regional scale that would be directly usable compared to those provided by GCMs. By systematically evaluating regional climate downscaling techniques, it also aims to provide a solid scientific basis for impact assessments. Last but not least, it aims to promote interaction and communication between the Global Climate Modelling community, the Regional Climate Modelling community and end users to better support adaptation activities (Giorgi et al., 2009).

The CORDEX initiative (Giorgi et al., 2009) has primarily focused their effort into downscaling CMIP5 GCMs (150-200 km resolution) using RCMs at 50 km (CORDEX-44) resolution. As computational resources have become more available, resolutions in RCMs have been further increased to 12 km (CORDEX-11) over Europe (Jacob et al., 2014; Kotlarski et al., 2014; Vautard et al., in prep) and 25 km (CORDEX-22) over other domains of the globe. This effort follows the CORE protocol (<https://www.cordex.org/experiment-guidelines/cordex-core>) and aims to provide a core set of comprehensive and homogeneous regional climate projections across many domains that can support IPCC AR6 assessments, to investigate the impact of model resolution, and to better constrain the model ensemble spread (Gutowski et al., 2016). The horizontal resolutions of 12 km over Europe and 25 km over all domains were chosen as a compromise between what is computationally possible for different modeling groups and the expected added value compared to GCMs. These community efforts within CORDEX have proved to be very useful to provide reliable climate information in terms of temperature, precipitation, winds mean and extremes (e.g. Kotlarski et al., 2014; Prein et al., 2016; Glisan et al., 2019), as well as their projected climate change signals over different parts of the globe (e.g. Gao et al., 2008; Jacob et al., 2014; Rajczak and Schär, 2017). Overall, RCMs have been shown to improve the representation of mean climate compared to their driving GCMs, particularly over orography according to their higher resolutions (Torma et al., 2015; Giorgi et al., 2016; Sørland et al., 2018). When the RCM resolution is refined from 50 km to 12 km, there is an improvement in terms of spatial and temporal distributions, particularly in mean and extreme precipitation in mountainous regions (Torma et al., 2015; Prein et al., 2016) due to its improved representation of orography. Summer seasons also tend to be better simulated in CORDEX-11 because the larger scales of convection are captured by the better resolved-scale dynamics (Prein et al., 2016). In addition, CORDEX-11 improves over CORDEX-44 in simulating amplitudes and historical trends of far extreme fall “mediterranean events”, which have increased in intensity of about 20% in the past 60 years or so (Luu et al., 2018). Overall, however, climate mean and variability do not change significantly by going from 50 to 12 km (e.g. Kotlarski et al., 2014; Casanueva et al., 2016; Jury et al., 2019).

Whether it is at 50 or 12 km resolution, the quality of RCM simulations has been shown to be linked to the internal skill of the RCM itself, which can be assessed by evaluating reanalysis-driven simulations (e.g. Kotlarski et al., 2014), but also to the quality of their driving GCMs (Giorgi and Mearns, 1999; Rummukainen, 2010; Diaconescu and Laprise, 2013; Hall,



2014). In the mid-latitudes, particularly in the winter season, RCMs strongly depend on the large-scale mean flow of the GCMs, which may negatively influence the RCM results (Hall, 2014; Kjellström et al., 2016; Brogli et al., 2019; Fernandez et al., 2019), although RCMs tend to correct some of the biases seen in their driving GCMs (e.g. Guo and Wang, 2016; Sørland et al., 2018). In other regions (e.g. in the Tropics) or in other seasons, local-scale processes can be more important than large-scale drivers and the uncertainties of RCM simulations are therefore less linked to their driving GCMs. For example, summer convection contributes largely to regional water budgets, particularly precipitation extremes, where RCMs' ability to simulate these events have been demonstrated (Prein et al., 2016). Radiation or surface wind speed biases of RCM simulations downscaling GCMs were clearly driven by RCM biases and GCMs appear not to contribute (Vautard et al., 2019). The argument that RCMs are performing poorly because of unrealistic large-scale circulation in the GCMs has unfortunately not facilitated the communication between the two communities (Schiermeier, 2010; Kerr, 2011, 2013), which have continued to evolve on separate paths. This dependency may be relaxed by the recently developed 2-step nesting convection-resolving model simulations (e.g. 2-4 km resolution) and many studies have already shown their advantages (Prein et al., 2013; Ban et al., 2015; Prein et al., 2015; Giorgi et al., 2016; Berthou et al., 2018; Schär et al., 2019). Although these convection-resolving simulations can be run at decadal scale, they are still too expensive to provide multi-model ensembles of centennial climate change projections and end users therefore have to rely on CMIP and CORDEX projections for adaptation activities.

In parallel to the development of the RCMs, GCMs have mainly been developed in terms of complexity, by adding more components of the Earth System into the models. Over the past decade, resolutions in GCMs have also increased from about 300 km for CMIP3, used in the 4th Assessment Report (AR4; Randall et al., 2007) of the Intergovernmental Panel on Climate Change (IPCC) to about 150 km for CMIP5, used in AR5 (Flato et al., 2013). CMIP6 (Eyring et al., 2016), which are analysed in the coming AR6, have recently been completed at about 100 km resolution. These large simulation ensembles have been extensively evaluated (e.g. Kumar et al., 2014) and their projections taken into consideration for the various IPCC Assessment Reports. A new high-resolution model intercomparison project, HighResMIP (Haarsma et al., 2016), has recently emerged due to the constant progress in computing power. HighResMIP calls for atmosphere and coupled GCMs at resolutions of 50-25 km, in addition to more standard CMIP-type resolutions, in order to understand the role of horizontal resolution in global climate simulation for model mean bias, variability and extremes. HighResMIP simulations have just finished and analyses on the role of resolution in these ensembles are currently underway. The benefits of resolution in GCMs have been investigated in the past in a non-coordinated way with single or small groups of models (e.g. Jung et al., 2012; Kinter III et al., 2013; Mizielinski et al., 2014), and have drawn similar conclusions regarding the emergence of weather-type systems that feedback on the global climate system. For example, increasing resolution in GCMs plays a role in the simulation of the global hydrological cycle (Roberts et al., 2018), which tends to be more intense but partitioned more realistically over land and ocean compared to observations due to stronger transport of atmospheric moisture (Demory et al., 2014) and a better representation of orography (Vannière et al., 2019). Coupling the atmosphere



135 with ocean eddy-permitting models tends to improve the climate mean state and variability (e.g. Minobe et al., 2008;
 Shaffrey et al., 2009; Roberts et al., 2016). Synoptic-scale dynamics are better resolved in GCMs with increasing resolution,
 which improves the representation of mid-latitude eddy-driven jet variability, extra-tropical cyclones and associated extreme
 precipitation (Catto et al., 2010; Haarsma et al., 2013; Schiemann et al., 2018; Baker et al., 2019), as well as blocking events
 (Matsueda and Palmer, 2011; Berckmans et al., 2013). Intensity of tropical cyclones in GCMs also increases with resolution,
 140 and their interannual variability is better captured (e.g. Zhao et al., 2009; Roberts et al., 2015), but the resolution in GCMs is
 still not high enough to capture the most intense tropical cyclones. All these weather-type processes can affect regional
 climate variability (e.g. Haarsma et al., 2013), so better simulating them can potentially lead to more realistic climate
 information and trustworthy climate change projections at the regional scale (e.g. Matsueda and Palmer, 2011). This question
 would be particularly important in regions where the water budget is partly driven by synoptic systems, such as tropical
 145 cyclones over East Asia (e.g. Guo et al., 2017) and Central America (e.g. Franco-Diaz et al., 2019), frontal systems and
 eddy-driven jet interactions with topography over Europe (e.g. Woollings et al., 2010; Catto et al., 2012; Baker et al., 2019).

There are currently two sets of RCM and GCM ensembles at similar resolutions: the 12-50 km CORDEX RCMs and the 25-
 50 km HighResMIP GCMs. So far, assessing the effect of increasing resolution in RCMs and GCMs have been performed
 150 compared to their lower resolution counterparts. With HighResMIP and CORDEX, it is the first time that GCM and RCM
 climate ensembles can be assessed against each other. Two questions emerge: 1) Can high-resolution GCMs reach the level
 of regional climate information that is provided by state-of-the-art RCMs, developed at higher resolution than state-of-the-art
 GCMs and specifically calibrated to simulate the climate of the region of interest? 2) Can we better constrain the spread of
 information by considering various model sources? Considering these two ensembles together would give some insights for
 155 planning future climate ensembles to improve climate projections and risk assessments at the regional scale.

In this study, we make use of the various RCM and GCM coordinated efforts (CMIP, CORDEX, HighResMIP) to
 investigate the spread of information given by various products, whether they are from low-resolution GCMs (CMIP5), high-
 resolution GCMs (HighResMIP), low-resolution RCMs (EUR-44) and high-resolution RCMs (EUR-11). We would like to
 160 determine for instance whether HighResMIP GCMs, due solely to their increasing resolution, provide information at the
 regional scale that is comparable to CORDEX. In other words, is the potential improvement of large-scale drivers of
 European climate with high resolution GCMs as beneficial as the local tuning of regional models? This would enable us to
 inform end users on the kind of information they can expect by considering different products. We focus our efforts on the
 daily precipitation distribution over European regions under current climate conditions. Section 2 presents the data used as
 165 well as the method employed to evaluate the daily precipitation distribution. Section 3 presents the results and includes
 various sensitivity tests related to the impact of resolution and the effect of regridding model data on coarser grids. Section 4
 presents several sensitivity tests regarding the method itself. Section 5 discusses the results and concludes with an opening
 towards the need for RCM and GCM communities to strengthen collaboration and communication.



2 Method and data

2.1 PRIMAVERA GCMs

We use the ocean-atmosphere coupled GCMs developed and run within the EU-Horizon 2020 PRIMAVERA project (<https://www.primavera-h2020.eu>), which is a European contribution to HighResMIP. PRIMAVERA uses the HighResMIP protocol (Haarsma et al., 2016), which is different from CMIP (e.g. different aerosols; refer to Haarsma et al., 2016, for details). As PRIMAVERA simulations are still running, we use the ones which were available at the time of the study. So far, PRIMAVERA simulations consist of 6 GCMs (Table 1). Most high-resolution simulations include one member only, but in case there are more (such as the IFS-HR that provides 6 members), we consider one per model in order to apply equal weights to each model.

2.2 CORDEX RCMs

Over Europe, we use the CMIP5-driven EUR-44 and EUR-11 CORDEX simulations (please refer to the EURO-CORDEX simulation list here: <https://euro-cordex.net/imperia/md/content/csc/cordex/20180130-eurocordex-simulations.pdf>) run at 0.44° (about 50 km) and 0.11° (about 12 km) resolution. Daily precipitation model data have been extracted from the Earth System Grid Federation (ESGF) servers (as summarised in Table 2). We focus our analysis on the EUR-44 simulations because their resolution roughly corresponds to the resolutions used by PRIMAVERA GCMs, which allows a clean comparison between the two ensembles. However, we evaluate the roles of resolution, regridding, and ensemble size in daily precipitation distribution with equivalent pairs from EUR-11.

2.3 CMIP5 GCMs

To investigate the added value of CORDEX RCM simulations to CMIP5 GCMs, we constrain our study to the subset of CMIP5 GCMs used to force CORDEX simulations (Table 2, second column), available on the ESGF servers. However, we examine the robustness of our findings by also analysing the entire ensemble of CMIP5 simulations. Taking the full set changes the ensemble spread but the main conclusions of the study regarding CMIP5 remain the same (not shown).

We perform our analysis either on the full CORDEX and PRIMAVERA ensembles or on reduced ensembles. Reduced ensembles correspond to PRIMAVERA GCMs and CORDEX RCMs that downscale CMIP5 GCMs that are based on the same GCM family, for example the PRIMAVERA MPI-ESM1-2-XR GCM and the EUR-44 RCA4, CCLM4, CCLM5 and REMO2009 that downscaled MPI-ESM-LR (blue colored in Table 2). Also, within CORDEX, a reduced ensemble (dark shaded in Table 2) is defined to compare results from EUR-44 and EUR-11.



2.4 Observations

Over Europe, we make use of the best available observational datasets (Fig. S1). These are mostly national datasets, such as SAFRAN-V2 (France; Vidal et al., 2010), UKCPobs (British Isles; Perry et al., 2009), ALPS-EURO4M (Alps; Isotta et al., 2014), CARPACLIM (Carpathian region; Szalai et al.). To cover the Iberian Peninsula, we combine Spain02 v2 (Herrera et al., 2012) and PT02 v2 (Belo-Pereira et al., 2011). For other regions, we considered E-OBS v17 (Cornes et al., 2018). E-OBS use the complete observational stations network for Scandinavia, Netherlands, Germany (Gerard van der Schrier, personal communication). E-OBS is therefore expected to have good quality over these regions. For the remaining regions, such as the Mediterranean region and the Eastern Europe, we also make use of E-OBS, although the quality is most likely lower (Prein and Gobiet, 2017). All the observation datasets used are listed in Table 3.

The advantage of using such national datasets are that they are available at high resolutions (5-20 km) and they contain a very dense stations network, which minimizes the effect of precipitation undersampling (Prein and Gobiet, 2017). These data are therefore considered to be the best available over Europe. Nevertheless, there are drawbacks, particularly related to the lack of precipitation undercatch correction. This issue can be particularly important for falling snow over mountains but also in other places when associated with strong winds (rain does not fall vertically in the gauges, which creates an error depending on wind speed and drop size). The lack of correction can include errors of 3-20% on average and up to 40-80% in high latitudes and mountainous regions (Prein and Gobiet, 2017). To overcome this problem, we use a method similar to Kotlarski et al. (2014) and Rajczak and Schär (2017), and assume a mean estimate of the undercatch error of 20% over all regions. All observations are therefore scaled by a factor of 1.2 over all grid points and over the entire time series, which gives us a rough estimate of observational uncertainties. We refer to it as a synthetic observational dataset.

Moreover, Prein and Gobiet (2017) advised to consider as many observational datasets as possible for regional analyses. Most datasets, however, are available either at much lower resolution than 50 km and therefore cannot be used for evaluating the ensembles at such resolution, or they are not available at daily timescales. We have done a test using GPCP v2 available daily at 1 degree resolution. The distribution shows almost no intense precipitation over most regions and in most seasons (not shown).

2.5 Period

To match the observation time periods with the PRIMAVERA and CORDEX ensembles, we focus our analyses on the present-day 1971-2005 over Europe.

2.6 Domains

We divide the European domain into subregions according to the areas covered by national observational datasets (Fig. S1). Over the sub-regions covered by E-OBS, we consider the PRUDENCE regions (Christensen and Christensen, 2007). Throughout the paper, we therefore refer to AL for the Alps, BI for British Isles, FR for France, CA for Carpathians, CE for



Central Europe, EE for East Europe, IP for Iberian Peninsula, MD for Mediterranean basin, NEE for Northeast Europe, SC for Scandinavia.

230 2.7 Description of precipitation distribution analysis

We look at the daily precipitation distribution in each sub-region (Fig. S1). We use a similar method as Berthou et al. (2019) based on the ASoP1 diagnostics tool developed by Klingaman et al. (2017). We calculate the daily precipitation distribution in terms of the actual contribution from 100 different intensity bins to mean precipitation. In order to account for the high frequency of low intensity precipitation events and the low frequency of high intensity events, we use an exponential bin distribution, as described by Berthou et al., 2019 (see their Fig. S5). To calculate the contribution to mean precipitation, each bin frequency is multiplied by its average rate. This way, mean precipitation is split in different contributions of different rates. We consider a logarithmic scale on the x-axis, so the area under the curve is directly proportional to the mean. Fig. 1 shows the resulting distribution for PRIMAVERA, EUR-44 and observations over the British Isles region (refer to Fig. S1 for the domain) in summer (JJA). Note that this type of histogram contains both information about mean precipitation (the area under the curve) and precipitation distribution. In this example, we see that EUR-44 tend to simulate more mean and intense summer precipitation over the UK, while PRIMAVERA has a lower mean, which is closer to observations for this area. However, PRIMAVERA tend to simulate too much drizzle precipitation (a common bias among GCMs; Dai, 2006; Stephens et al., 2010), while EUR-44 does not simulate such behaviour and is therefore closer to observations. These results are summarised in the pie plot (right panel of Fig. 1) for all seasons (DJF, MAM, JJA, SON).

245 The intercomparison of the model ensembles is performed as follows:

- 1) All datasets are regridded on the EUR-44 rotated pole grid, using a first-order conservative remapping. Then the precipitation data is pooled from each region and season. This step is repeated for every model and observational dataset.
- 250 2) The ensemble mean is calculated for each bin and a bootstrap resampling is used 1000 times on each model ensemble (CORDEX and PRIMAVERA) to establish a confidence interval around the ensemble mean (the 10% confidence interval is plotted with shaded colours around the ensemble mean in Fig. 1). For the observations, the bootstrap resampling is done on single years, therefore reflecting inter-annual variability.
- 3) A p -value is calculated on the difference between the two ensembles for each bin (plotted in grey crosses in Fig. 1). We apply a 10% threshold on each bin to validate that the two ensembles are significantly different (p -value < 0.1).
- 255 4) We group the bins as 3 intensity precipitation intervals (low: 1-10 mm/day; mid: 10-60 mm/day; high: >60 mm/day). We evaluate for each interval the percentage of bins over which they differ.
- 5) If the ensembles differ by more than 90% over that interval, the part of the pie corresponding to the season, region and precipitation interval is coloured (Fig. 1, right panel).



260 6) If the ensembles differ by more than 90%, we determine which one is less significantly different from the
 observations using the same metric between the observational spread (inter-annual variability) and each ensemble
 spread. If an ensemble has at least 10% less difference with the observations than the other, then its first letter is
 added to that part of the pie (P and C stand for PRIMAVERA and CORDEX, respectively). If the two ensembles
 are both close to observations (both differ by less than 30% with the observations), then we add an “=” sign to the
 265 pie section.

These steps are performed for every season, region and intensity interval, and plotted as shown in Fig. 1. The pie plot is
 therefore a way to synthesize information for the comparison between CORDEX and PRIMAVERA (section 3.3).

We focus our analyses on DJF (December-February) and JJA (June-August), which show the largest differences. The
 intermediate seasons, MAM (March-May) and SON (September-November) have also been analysed but are not discussed
 270 in details, as their results were usually similar to DJF and JJA depending on the season and the regions.

Computation of p-values. *P*-values are computed following Berthou et al. (2019) and Kendon et al. (2019). *P*-values are
 estimated for each bin as follows: 1) for each bin, the difference in precipitation contribution is calculated 1000 times using a
 bootstrap resampling (performed on the ensemble for the models, and the inter-annual variability for the observations); 2) the
 275 mean of the bootstrapped metric is computed, and subtracted from each 1000 bootstrap estimates; this creates 1000 zero-
 centred metrics and gives us an estimate of the probability distribution of the test statistic under the null hypothesis that the
 two ensembles are the same; 3) the original metric is then compared with this null distribution, and the *p*-value is estimated
 based on which quantile the original metric corresponds to relative to the null distribution. For instance, if the original metric
 is below 2% or above 98% of the values in the simulated null distribution, the uncorrected *p*-value would be 0.02.

280 The bootstrap resampling gives a spread of ensemble means, and not of models themselves. Because PRIMAVERA has only
 6 models, some of the means of the bootstrap resampling will be close to individual model behaviour, so the ensemble
 spread of the bootstrap can be relatively larger than with the 26 CORDEX models, where the bootstrap resampling is much
 less likely to pick individual models. What we are assessing with the bootstrap resampling is whether the ensemble means
 285 are different if we resample the models within them.

The resampling in the observations is done on inter-annual variability but the bootstrapping also represents a spread of
 averages, which is directly comparable with the spread of ensemble means, rather than comparing inter-annual variability
 with inter-member spread directly through standard deviations. We show that the main conclusions are not sensitive to the
 use of bootstrapping or interquartile range in section 3.4.

290 2.8 Sensitivity analyses

In order to evaluate the robustness of our results, we have performed several sensitivity analyses to evaluate:

- the role of regridding by comparing EUR-11 results on their native grid or regridded on the EUR-44 grid



- the role of model ensemble size by comparing all models versus a reduced ensemble
- the sensitivity of the results to the bootstrapping methodology by considering an inter-quartile (25%-75%) ensemble spread
- the sensitivity of the results to the significance threshold by considering p -value=0.01, 0.05 and 0.1 on different percentages of each interval.
- the sensitivity of the results to the definition of the bins (size and distribution)

These analyses are discussed in Section 4 of the manuscript.

300 3 Results

3.1 Precipitation distribution in CORDEX and CMIP5 ensembles

Fig. 2 and 3 show the precipitation distribution for EUR-44, EUR-11, and a selection of CMIP5 GCM models. The selection corresponds to the subset of GCMs that were downscaled by EUR-44 and EUR-11 RCMs: CNRM-CM5, CSIRO-Mk3-6-0, EC-EARTH (2 members), GFDL-ESM2G, GFDL-ESM2M, HadGEM2-ES, IPSL-CM5A-LR, IPSL-CM5A-MR, MIROC5, MPI-ESM-LR (2 members), NorESM1-M (refer to Table 2).

All data are plotted on the models native grid but use a common mask to define the regions regridded on each model grid. The British Isles region is not included because the resolutions of most CMIP5 GCMs are too low for significant results. Moreover, here we only focus on the differences between CORDEX and CMIP5, so observations are not included.

In Winter (Fig. 2), there is a clear shift in the precipitation distribution going from CMIP5 to CORDEX (EUR-44 and EUR-11) over all regions (results from other regions can also be seen in Fig. S2). EUR-44 and EUR-11 simulate an overall decrease in low intensity precipitation and an increase in high intensity precipitation. Moreover, EUR-11 tend to show a decrease in mid-rate precipitation compared to EUR-44. The shift towards more intense precipitation can be seen in all regions but is particularly clear over coastal and orographic regions (MD, SC, AL, IP), which is presumably attributed to the increase in resolution (Prein et al., 2016).

In Summer (Fig. 3), these findings are still valid between CMIP5 and CORDEX. CMIP5 simulate very little high intensity precipitation, while their mid-rate precipitation is much larger than CORDEX. This finding may be attributed to the finer grid box (meaning the rain rates are those of a smaller area), the better representation of orography and coastlines that may enhance the triggering of summer convective precipitation, the use of convective schemes which are more appropriate at the resolution of the RCMs, or the tuning of parameterization schemes. The differences between EUR-44 and EUR-11 are reduced, which suppose that such resolution jump does not influence summer precipitation largely when convection parameterization is used. This is also seen in other regions (Fig. S3), and is in line with previous studies showing no systematic improvement between EUR-44 and EUR-11 for mean precipitation (Kotlarski et al., 2014, Casanueva et al.,



2016). The effect of resolution remains, however, large for summer precipitation over orography (e.g. AL), which confirms the findings of Torma et al. (2015) and Prein et al. (2016).

Analyses have also been performed on all CMIP5 GCMs available on ESGF (not shown). We have found that the ensemble mean (area under the curve) is slightly lower when considering all CMIP5 models, but the distribution does not shift, so our above conclusions do not change.

3.2 Precipitation distribution in CORDEX and PRIMAVERA ensembles

When comparing EUR-44 and PRIMAVERA (Fig. 4 and 5), we find that the two ensembles are relatively similar, as opposed to how CORDEX compares with CMIP5 (Fig. 2 and 3). The effect of resolution is therefore the most important aspect to capture a realistic distribution of daily precipitation contribution to each rain rate. Overall there is no systematic difference between CORDEX and PRIMAVERA, but the two ensembles show different distributions, depending on region and season.

As for CMIP5, PRIMAVERA still overestimate low intensity precipitation in all seasons and regions, although to a lesser extent. In summer, PRIMAVERA have significantly less heavy rain rates than EUR-44 in all regions, which is more in agreement with observations, but both are within the observational range when considering a 20% rainfall undercatch (Fig. 5). PRIMAVERA also tend to simulate mid rain rates closer to observations in winter (Fig. 4) and transitional seasons, but this is mostly because of a sub-selection of GCMs within PRIMAVERA, except in the centre and east of the domain when conclusions are robust to the reduced ensemble. Heavy precipitation tends to be lower than EUR-44. When compared to observations, PRIMAVERA tend to be more realistic in the mid and heavy rain rates. However, when considering a 20% undercatch error, this is not systematically true, particularly for the most intense rain rates in JJA (Fig. 5).

To summarise our results, we have gathered the precipitation distribution comparisons onto a common figure, as explained in section 2.7. Figure 6a shows the results of the comparison of the two ensembles for each region, season and bin rate interval (low/mid/heavy rain rates). Fig. 6b shows the same figure but for the ensembles reduced to the GCM families shared by the ensembles (4 GCMs, 17 RCMs, see Table 2).

For all regions, EUR-44 and PRIMAVERA ensemble means significantly differ (the part of the pie is coloured) from each other for the most intense rainfall rates in summer (JJA). EUR-44 indeed generally show a heavier precipitation tail in all regions, which is often significantly larger than PRIMAVERA (e.g. IP, CA and AL regions; Fig. 5). PRIMAVERA shows less contribution from these strong precipitation events, in better agreement with the observations in most regions except the Alps. This conclusion is the most robust one and remains true when the strictest criteria of difference is applied (Fig. 7 top right corner). In the Alps, the heavy precipitation tail tends to be overestimated by CORDEX and underestimated by PRIMAVERA, so observations lie in between the two ensembles. However, when a 20% undercatch error in the



observations is assumed, EUR-44 are closer to the observed estimate (dashed line in Fig. 5 and Fig. S5). In other seasons, EUR-44 also have significantly larger contributions from intense precipitation compared to PRIMAVERA in many regions. They are in general further away from observations but closer to the synthetic observations accounting for precipitation undercatch.

When the same GCMs are used (Fig. 6b), the differences in the medium bins are only found in the centre or east of the domain (FR, CE, CA), which is potentially where EUR-44 are less influenced by the boundary conditions provided by the GCMs. In these regions, PRIMAVERA tend to simulate less contribution from these medium bins. This is in better agreement with the observations, even if the 20% undercatch error is taken into account (Fig. 4 and Fig. S4).

Both ensembles are the furthest away from the observations for the medium rain rates in winter (Fig. 4 and S4) and in spring (not shown), mostly overestimating precipitation. They are in best agreement with the observations in summer and autumn for these bins (Fig. 5 and S5), except in the CA region where they both underestimate summer rainfall.

4 Sensitivity tests on the method

4.1 Sensitivity of results to significance thresholds

To determine whether our main results shown in the pie charts depend on the chosen significant thresholds, we have performed sensitivity analyses to: 1) the threshold that defines the level of significance (p -value of 10, 5 or 1%); 2) the percentage of the interval on which bins are significantly different (50, 70 or 90%). The results are summarised in Fig. 7. For the most relaxed criteria (bottom left panel), the ensemble means of EUR-44 and PRIMAVERA are different in most seasons and bins, except in winter where the ensembles are more similar in regions SC, BI, IP and MD. With a strict criteria (top right panel), the two ensembles show a similar distribution. Significant differences between the two ensembles mostly remain for heavy precipitation in summer in all regions, as well as in CE, BI, CA in all seasons. There are significant differences also for medium rainfall in BI, CE and CA in at least two seasons. The Alps is a region which is quite sensitive to the threshold definitions, particularly in summer regarding the comparison between the ensembles and the observations. This is because observations lie in between PRIMAVERA and CORDEX for most rain rates (Fig. 5). However, the pie charts do not consider the possible observational precipitation undercatch error, which would benefit EUR-44 in this region. The observations quality is therefore of particular importance in orographic regions such as the Alps. The distribution for the lowest rain rates in CORDEX is generally close to the observed distribution, while PRIMAVERA tend to have too large contribution from low intensity, as described earlier. This result, however, depends on the threshold value. For relaxed thresholds (bottom left panels), the two ensembles differ more compared to strict thresholds (top and right panels).



4.2 Sensitivity of results to bin definitions

Fig. S6 shows the same pie charts but using different underlying bin definitions: exponential distribution with 100 bins, 200 bins, or a regular 1 mm/day bin definition (Berthou et al., 2019). The results are weakly dependent on the bin definition, except for the Alps and the Mediterranean regions, for which more precipitation intervals are different when using the regular bin definition. Regular bins also favour EUR-44 in the Alps in summer (as discussed in the previous paragraph).

4.3 Sensitivity of results to the bootstrap method

We chose to use a confidence interval based on bootstrapped ensembles. We therefore analyse the variability of the ensemble mean when the ensemble is randomly changed rather than the intermember spread itself. We argue that this method allows a fairer comparison with the observation mean bootstrapped on interannual variability. Through this approach, we can evaluate if the ensemble means are significantly different, rather than if the ensembles themselves are different. To evaluate the sensitivity of our results to that choice, and assess the robustness of our conclusions from the pie charts, we also show the median and interquartile range of the distributions for PRIMAVERA, EUR-44, and the observations, each individual year being considered as “one member” (Fig. 8). We find that our first main result, the two ensembles differ for heavy precipitation in summer, are still valid: the median of PRIMAVERA is outside the interquartile range of EUR-44 above 60 mm/day in all regions. Our second conclusion, PRIMAVERA and EUR-44 (when driven by the same GCM family as PRIMAVERA) differ most in the centre of the domain, is also robust (e.g. Fig. S9 for winter).

4.4 Sensitivity of results to the choice of EUR-44 or EUR-11

We showed earlier (section 3.1) that EUR-11 and EUR-44 show similar distributions over most areas, except where there is complex topography (orography or coastal regions) and for intense precipitation. These results were shown on the models’ native grids. This analysis has the benefits of showing the actual ability of the models on their own grid, but it also takes into account technical aspects related to different land-sea contrasts that may include noise into the results. To further investigate the role of resolution in CORDEX simulations, we analyse the daily precipitation distribution for EUR-11, EUR-44 and observations on a common EUR-44 grid. These analyses also serve to assess the robustness of our results between PRIMAVERA and EUR-44 using a larger EUR-11 ensemble. The results are shown in Fig. 9 and 10 (as well as Fig. S7 and S8 for other regions). When shown on a common grid, we find that EUR-11 and EUR-44 show similar results, particularly in the low- to mid-rain rates. However, EUR-11 simulate more intense precipitation than EUR-44 over orographic and coastal regions, particularly in winter. There are differences whether EUR-11 are regridded on the EUR-44 grid or not (not shown), which are expected, but these results show that the main findings between PRIMAVERA and CORDEX still hold, even when considering EUR-11.



5 Discussion and conclusion

In this study, we have considered high-resolution (25-50 km) PRIMAVERA GCMs, following the HighResMIP protocol, and CORDEX RCMs (available at 12-50 km resolutions) present-day simulations to make an evaluation of their simulated daily precipitation distribution over Europe. This study is the first attempt to evaluate GCM and RCM ensembles provided at similar horizontal resolutions at the regional scale.

Our results show that CMIP5-driven EUR-44 and PRIMAVERA atmosphere-ocean coupled simulation ensembles give equivalent regional climate information in terms of daily precipitation distribution and its contribution to precipitation intervals. The differences in their precipitation distribution are generally small (Fig. 4-5) and much smaller than differences between CORDEX and CMIP5, where the value of CORDEX is indisputable (Fig. 2-3). CMIP5 model ensemble show rather different distributions, particularly shifted to smaller precipitation intensities, as expected from their coarse grids. PRIMAVERA and CORDEX ensembles are of good quality in summer and autumn (except in the CA region), but tend to overestimate precipitation in winter and spring. However, there are some precipitation intervals, seasons and regions for which the two ensembles significantly differ. A large difference between the two ensembles is found for heavy precipitation (in all regions in summer, and in some regions in other seasons). PRIMAVERA have less heavy rainfall than EUR-44, and tend to agree better with raw observations, while EUR-44 are closer to synthetic observational datasets when a 20% undercatch error is considered. Moreover, EUR-11 partially correct this overestimation of heavy precipitation seen in EUR-44. European summer precipitation is mostly driven by local convective precipitation, which is not explicitly simulated in state-of-the-art RCMs and GCMs. At such resolutions (at best 12 km), convection is parameterized. In RCMs, such parameters are commonly set by expert tuning or objective calibration to simulate a mean climate as close as possible to observations over the region of interest in hindcast simulations (using reanalysis boundary forcing; e.g. Bellprat et al., 2016). It is not possible to perform such tuning in GCMs. GCMs are commonly tuned to balance top-of-the-atmosphere radiation globally or to better represent specific processes, but cannot be tuned over a specific region (Hourdin et al., 2017). A hypothesis to explain this excess in rainfall in the CORDEX ensemble is that most RCMs do not use the semi-implicit semi-Lagrangian numerics commonly used in GCMs that allow for longer time steps. Using shorter time steps tends to increase both mean and extreme precipitation (C. Zeman, personal communication). PRIMAVERA GCMs tend to have more light precipitation than EUR-44, and too much compared to the observations, although this result is not as robust as the former one. It is possible that expert tuning of the convective scheme and land-surface scheme in RCMs has a positive effect towards reducing this “drizzling” problem.

The advantage of EUR-11 over EUR-44 is mostly found in winter, when precipitation strongly depend on the interaction of large-scale circulation with orography. Otherwise the differences are rather small when aggregated over a region (Fig. 9-10).



450 Another conclusion is that when considering only shared GCM families between the two ensembles, differences in the bulk of the distribution (medium rain rates) is mostly found in the central and eastern parts of the European domain, in autumn, winter and spring (Fig. 6b). PRIMAVERA tend to reduce precipitation overestimation in these regions and seasons compared to EUR-44. This could be linked with better simulation of blocking frequency in PRIMAVERA GCMs (Schiemann et al., 2018), which is not achieved by CORDEX (Jury et al., 2019).

455 Finally, some conclusions are specific to a few regions: over the Alps and the British Isles, PRIMAVERA underestimate heavy precipitation in summer while EUR-44 overestimate it, although EUR-44 is in good agreement with a rough correction of precipitation undercatch (rain rates increased by 20%). Over the British Isles, precipitation over 30 mm/day is underestimated in autumn, winter and spring by both ensembles. This could mean that those models are still too coarse to
 460 correctly represent the interactions between low pressure systems and local coastal and orographic effects over this region. In the Carpathians, summer precipitation is underestimated by both ensembles and winter precipitation is overestimated, although PRIMAVERA brings some improvements in this case.

These results are based on the model ensembles of PRIMAVERA and CORDEX. Different conclusions may be drawn either
 465 when evaluating models individually (e.g. Klingaman et al., 2017, show large differences in the character of rainfall in different models) or with a slightly different selection of models within the ensembles. To evaluate the spread of the results when selecting different models within the ensembles, we have therefore used a bootstrap resampling method applied 1000 times on each ensemble. For comparison, we have also used an interquartile range to evaluate the spread of each ensemble (section 4.3), as well as models individually (not shown). We have also performed several sensitivity tests to assess the
 470 robustness of our results to the choice of the bin distribution, to the significance threshold, to the models' grid (native or common). The main conclusions summarised above still hold.

This study is a first effort to evaluate the quality of regional climate information provided by GCM and RCM ensembles of similar horizontal resolutions. We have only investigated daily precipitation distribution, and such an exercise needs to be continued with other fields (temperature, winds) mean, variability and extremes. Nevertheless, the results are very
 475 promising, in particular as the two ensembles have similar performance. PRIMAVERA and CORDEX, being EUR-11 or EUR-44, should therefore be considered equally credible, depending on the user's needs, such as those aggregated over a domain. For studies at the local scale or over orography, however, a higher resolution model dataset, such as EUR-11, would inevitably give more detailed spatial information (e.g. Kotlarski et al., 2014; Prein et al., 2015).

The performance of PRIMAVERA was not logically expected because these GCMs were developed at a coarser resolution,
 480 and only their resolution was increased. The tuning was performed on their low-resolution counterparts, so little additional tuning was performed at these high resolutions (see Roberts et al., in revision, for changes in models when increasing resolution), as opposed to RCMs which are developed at a higher resolution and potentially tuned at each resolution.



485 The fact that PRIMAVERA results exhibit moderate improvements over CMIP5-driven CORDEX simulations for precipitation over Europe is also an important result of this study, which is consistent with the results of Iles et al. (2019) who used a very different method to compare GCMs and RCMs at different resolutions. It indicates that the potential improvement of large-scale dynamics in GCMs due to higher resolution does not have a strong influence on precipitation improvement, which is largely driven by downscaling.

490 The added value of RCMs to CMIP5 GCMs is also an important result, and it emphasizes the importance of a well designed, well evaluated model chain when using dynamical downscaling as a method to obtain higher resolution climate data. We show here that considering climate information from various sources is crucial.

We have also taken into account the issue associated with observational uncertainty. To try to reduce as much as possible uncertainties linked to observations, we have used national gridded observational datasets. Although of very high quality, these are still not fit for a thorough evaluation of climate models at the regional scale, particularly over orography, and we
495 had to roughly correct the observations by adding an averaged 20% to account for precipitation undercatch. This is not ideal but believed to be fairer when evaluating higher resolution models.

In this study, we have only focused on present-day simulations. Assessing future climate projections between the two ensembles may be more difficult because the results would depend on other parameters independent of the models
500 themselves, such as the lack of a common protocol (e.g greenhouse gases and aerosols forcings) between RCMs and GCMs. Assessing the impact of aerosol forcings on the climate projections is currently being investigated (Boé et al., in revision; Gutierrez et al., in revision).

We have limited our study to Europe, which has the advantage of having a large RCM ensemble. In the future, this work should be extended to other regions of the world, where CORDEX-22 and CORDEX-44 ensembles can be assessed with
505 HighResMIP GCMs.

6 Code availability

The code used for the analyses presented in this manuscript is developed by Berthou et al. (2019) available under the terms of the Apache 2.0 license from <https://github.com/PRIMAVERA-H2020/PrecipDistribution> (DOI: 10.5281/zenodo.3666302). This code uses the method that computes precipitation histograms of the contributions of specific
510 intensity bins to the total precipitation based on the ASoP1 diagnostics developed by Klingaman et al. (2017) and available under the terms of the Apache 2.0 license from <https://github.com/nick-klingaman/ASoP>.



7 Data availability

All PRIMAVERA and CORDEX model data used in this study can be obtained from the Earth System Grid Federation nodes, such as esgf-data.dkrz.de, esgf-index1.ceda.ac.uk, cordexesg.dmi.dk, esgf-node.ipsl.fr, and esg-dn1.nsc.liu.se. Note that the simulations are still being produced, so the ensembles presented in this article may not cover the whole ensembles available on the ESGF archive. For a complete list of EURO-CORDEX simulations, please refer to the EURO-CORDEX homepage (www.euro-cordex.net). Details about PRIMAVERA data availability can be found in Roberts et al. (2017), Roberts (2018), Scoccimarro et al. (2018), von Storch et al. (2018), EC-Earth Consortium (2019), Voldoire (2019). PRIMAVERA Persistent Identifiers (PID) and CORDEX file tracking IDs are listed in the Data folder of <https://github.com/PRIMAVERA-H2020/PrecipDistribution> (DOI: 10.5281/zenodo.3666302). Spain02 are available at <http://www.meteo.unican.es/datasets/spain02>; PT02 are available at <http://www.ipma.pt/pt/produtoseservicos/index.jsp?page=dataset.pt02.xml>. EURO4M-APGD are available at <https://www.meteoswiss.admin.ch/home/search.subpage.html/en/data/products/2015/alpine-precipitation.html> (doi: 10.18751/Climate/Griddata/APGD/1.0). CARPATCLIM are available at http://surfobs.climate.copernicus.eu/dataaccess/access_carpatclim.php. The E-OBS data are obtained through the ECA&D project: <https://www.ecad.eu>.

Author contributions. The authors list is written by contribution (from M-E Demory to C. Schär), then in alphabetic order. M-E Demory and S. Berthou ran the analyses on all models and observations used in this study, based on the diagnostics developed by S. Berthou and previously published. S. Sørland and M. Roberts contributed to CORDEX and PRIMAVERA analyses, respectively. U. Beyerle provided all CORDEX and CMIP5 data downloaded from ESGF. J. Seddon provided the PRIMAVERA data on CEDA JASMIN (Lawrence et al., 2013). R. Haarsma and C. Schär were strongly involved in the discussion of the results. The other co-authors contributed to run the simulations. M-E Demory wrote the manuscript, together with S. Berthou and S. Sørland, and with input from all other co-authors.

Acknowledgement. This work is funded through the EU Copernicus Climate Change Service (C3S): Producing Regional Climate Projections Leading to European Services (PRINCIPLES). The PRIMAVERA project is funded by the European Union's Horizon 2020 programme, Grant Agreement no. 641727. We acknowledge the World Climate Research Programme's Working Group on Regional Climate, and the Working Group on Coupled Modelling, former coordinating body of CORDEX and responsible panel for CMIP5. We also thank all the climate modelling groups (listed in Tables 1 and 2 of this paper) for producing and making available their model output. We also acknowledge the Earth System Grid Federation infrastructure, an international effort led by the U.S. Department of Energy's Program for Climate Model Diagnosis and Intercomparison, the European Network for Earth System Modelling and other partners in the Global Organisation for Earth System Science Portals (GO-ESSP).



Our group acknowledge PRACE for awarding us access to Piz Daint at ETH Zürich/CSCS (Switzerland) for conducting CCLM simulations. This work used JASMIN, the UK's collaborative data analysis environment (<http://jasmin.ac.uk>). We acknowledge the E-OBS dataset from the EU-FP6 project UERRA (<http://www.uerra.eu>) and the data providers in the ECA&D project (<https://www.ecad.eu>). We acknowledge the CARPATCLIM Database © European Commission - JRC, 2013. The authors thank IPMA for the PT02 precipitation dataset, as well as AEMET and UC for the Spain02 dataset, available at <http://www.meteo.unican.es/datasets/spain02>. The SAFRAN dataset was provided by METEO FRANCE. The European Climate Prediction system, which provided UKCPobs, is funded by the European Union's Horizon 2020 programme, Grant Agreement no. 776613. We thank the Federal Office of Meteorology and Climatology MeteoSwiss for providing the Alpine precipitation grid dataset (EURO4M-APGD) developed as part of the EU project EURO4M (www.euro4m.eu).

References

- Baker, A. J., R. Schiemann, K. I. Hodges, M.-E. Demory, M. S. Mizieliński, M. J. Roberts, L. C. Shaffrey, J. Strachan, P. L. Vidale (2019). Enhanced Climate Change Response of Wintertime North Atlantic Circulation, Cyclonic Activity, and Precipitation in a 25-km-Resolution Global Atmospheric Model. *J. Climate*, 32, 7763–7781, <https://doi.org/10.1175/JCLI-D-19-0054.1>
- Ban N., J. Schmidli, C. Schär (2015). Heavy precipitation in a changing climate: Does short-term summer precipitation increase faster? *Geophys. Res. Lett.*, 42, 1165–1172.
- Bellprat, O., S. Kotlarski, D. Lüthi, R. De Elia, A. Frigon, R. Laprise, C. Schär (2016). Objective calibration of regional climate models: Application over Europe and North America. *J. Climate*, 29, 819–838.
- Belo-Pereira, M., E. Dutra, P. Viterbo (2011). Evaluation of global precipitation data sets over the Iberian Peninsula, *J. Geophys. Res.*, 116, D20101, [doi:10.1029/2010JD015481](https://doi.org/10.1029/2010JD015481).
- Berckmans, J., T. Woollings, M.-E. Demory, P. L. Vidale, M. Roberts (2013). Atmospheric blocking in a high-resolution climate model: influences of mean state, orography and eddy forcing. *Atm. Sci. Lett.*, 14, 34–40.
- Berthou S., E. Kendon, S. Chan, N. Ban, D. Leutwyler, C. Schär, G. Fosser (2018). Pan-European climate at convection-permitting scale: a model intercomparison study. *Clim. Dyn.*, online, <https://doi.org/10.1007/s00382-018-4114-6>
- Berthou, S., Kendon, E., Rowell, D. P., Roberts, M. J., Tucker, S. O., Stratton, R. A. (2019). Larger future intensification of rainfall in the West African Sahel in a convection-permitting model. *Geophysical Research Letters*, 46, <https://doi.org/10.1029/2019GL083544>
- Boé J., Somot S., Corre L., Nabat P. Large differences in Summer climate change over Europe as projected by global and regional climate models : causes and consequences. *Clim. Dyn.*, in revision.
- Brogli, R., N. Kröner, S.L. Sørland, C. Schär (2019). Causes of Future Mediterranean Precipitation Decline Depend on the Season. *Env. Res. Letters*, in press, <https://doi.org/10.1088/1748-9326/ab4438>



- Casanueva, A., Kotlarski, S., Herrera, S., Fernández, J., Gutiérrez, J. M., Boberg, F., Colette, A., Christensen, O. B., Goergen, K., Jacob, D., Keuler, K., Nikulin, G., Teichmann, C., Vautard R. (2016). Daily precipitation statistics in a EURO-CORDEX RCM ensemble: added value of raw and bias-corrected high-resolution simulations. *Clim. Dyn.*, 47, 719-737
- 590 Catto, J. L., L. C. Shaffrey, K. I. Hodges (2010). Can climate models capture the structure of extra-tropical cyclones? *J. Clim.*, 23, 1621-1635.
- Catto, J. L., C. Jakob, G. Berry, and N. Nicholls (2012). Relating global precipitation to atmospheric fronts. *Geophys. Res. Lett.*, 39, L10805.
- 595 Cherchi, A., Fogli, P. G., Lovato, T., Peano, D., Iovino, D., Gualdi, S., Masina, S., Soccimarro, E., Materia, S., Bellucci, A., and Navarra, A. (2019). Global mean climate and main patterns of variability in the CMCC-CM2 coupled model. *Journal of Advances in Modeling Earth Systems*, 11, 185–209. <https://doi.org/10.1029/2018MS001369>
- 600 Christensen, J. H. and Christensen, O. B. (2007). A summary of the PRUDENCE model projections of changes in European climate by the end of this century. *Climatic Change*, 81, 7-30. <https://doi.org/10.1007/s10584-006-9210-7>
- Cornes, R. C., van der Schrier, G., van den Besselaar, E. J. M., Jones, P. D. (2018). An ensemble version of the E-OBS temperature and precipitation data sets. *J. Geophys. Res.: Atmos.*, 123, 9391–9409. <https://doi.org/10.1029/2017JD028200>
- 605 Dai, A. (2006). Precipitation characteristics in eighteen coupled climate models. *J. Clim.*, 19, 4605-4630.
- Diaconescu E. P. and Laprise R. (2013). Can added value be expected in RCM-simulated large scales? *Clim. Dyn.*, 41, 1769–1800. <https://doi.org/10.1007/s00382-012-1649-9>
- 610 Dickinson, R. E., R. M. Errico, F. Giorgi, and G. T. Bates (1989). A regional climate model for the western United States. *Climatic Change*, 15, 383–422.
- EC-Earth Consortium (EC-Earth) (2019). EC-Earth-Consortium EC-Earth3 model output prepared for CMIP6 HighResMIP hist-1950. Version 20181212. Earth System Grid Federation.
- 615 Eyring, V., Bony, S., Meehl, G. A., Senior, C. A., Stevens, B., Stouffer, R. J., and Taylor, K. E. (2016). Overview of the Coupled Model Intercomparison Project Phase 6 (CMIP6) experimental design and organization, *Geosci. Model Dev.*, 9, 1937-1958, doi:10.5194/gmd-9-1937-2016.
- 620 Fealy, R., Bruyere, C., Duffy, C. (2018). Regional Climate Model Simulations for Ireland for the 21st Century. Final Report submitted to the Environmental Protection Agency, Co. Wexford, pp. 1-137. ISBN: 978-1-84095-770-9
- 625 Fernández J., Frías M.D., Cabos W.D., Cofiño, A. S., Domínguez, M., Fita, L., Gaertner, M.A., García-Díez, M., Gutiérrez, J. M., Jiménez-Guerrero, P., Liguori, G., Montávez, J. P., Romera, R., Sánchez, E. (2019). Consistency of climate change projections from multiple global and regional model intercomparison projects. *Clim. Dyn.*, 52, 1139-1156. <https://doi.org/10.1007/s00382-018-4181-8>
- 630 Flato, G., J. Marotzke, B. Abiodun, P. Braconnot, S.C. Chou, W. Collins, P. Cox, F. Driouech, S. Emori, V. Eyring, C. Forest, P. Gleckler, E. Guilyardi, C. Jakob, V. Kattsov, C. Reason and M. Rummukainen (2013). Evaluation of Climate Models. In: *Climate Change 2013: The Physical Science Basis. Contribution of Working Group I to the Fifth Assessment Report of the Intergovernmental Panel on Climate Change* [Stocker, T.F., D. Qin, G.-K. Plattner, M. Tignor, S.K. Allen, J. Boschung, A. Nauels, Y. Xia, V. Bex and P.M. Midgley (eds.)]. Cambridge University Press, Cambridge, United Kingdom and New York, NY, USA.
- 635



- Franco-Díaz, A., Klingaman, N.P., Vidale, P.L., Guo L., Demory M.-E. (2019). The contribution of tropical cyclones to the atmospheric branch of Middle America's hydrological cycle using observed and reanalysis tracks. *Clim. Dyn.*, 53, 6145–6158, doi:10.1007/s00382-019-04920-z
- 640 Gao, X., Y. Shi, R. Song, F. Giorgi, Y. Wang, and D. Zhang (2008). Reduction of future monsoon precipitation over China: Comparison between a high resolution RCM simulation and the driving GCM. *Meteor. Atmos. Phys.*, 100, 73–86.
- Giorgi, F., and Mearns, L. O. (1999). Introduction to special section: Regional Climate Modeling Revisited, *J. Geophys. Res.*, 104, 6335–6352, doi:10.1029/98JD02072.
- 645 Giorgi, F., C. Jones, G. R. Asrar (2009). Addressing Climate Information Needs at the Regional Level: The CORDEX Framework. *WMO Bulletin*, 58, 175–183.
- Giorgi, F., C. Torma, E. Coppola, N. Ban, C. Schär, S. Somot (2016). Enhanced summer convective rainfall at Alpine high
 650 elevations in response to climate warming. *Nature Geosci.*, 9, 584–589. doi:10.1038/ngeo2761
- Giorgi, F. (2019). Thirty years of regional climate modeling: Where are we and where are we going next? *Journal of Geophysical Research: Atmospheres*, 124, 5696–5723. <https://doi.org/10.1029/2018JD030094>
- 655 Glisan, J. M., Jones, R., Lennard, C., Castillo Pérez, N. I., Lucas-Picher, P., Rinke, A., Solman, S., Gutowski Jr., W. J. (2019). A metrics-based analysis of seasonal daily precipitation and near-surface temperature within seven Coordinated Regional Climate Downscaling Experiment domains. *Atmos. Sci. Lett.*, 20, e897, <https://doi.org/10.1002/asl.897>
- Guo, D. L., and H. J. Wang (2016). Comparison of a very-fine-resolution GCM with RCM dynamical downscaling in
 660 simulating climate in China. *Adv. Atmos. Sci.*, 33, 559–570, doi: 10.1007/s00376-015-5147-y.
- Guo, L., N. P. Klingaman, P. L. Vidale, A. G. Turner, M.-E. Demory, A. Cobb (2017). Contribution of tropical cyclones to atmospheric moisture transport and rainfall over East Asia. *J. Clim.*, 30, 3853–3865.
- 665 Gutierrez, C., Somot S., Nabat P., Mallet M., Corre L., Van Meijgaard E., Perpiñán O., Gaertner M.A. Future evolution of surface solar radiation and photovoltaic potential in Europe : investigating the role of aerosols. *Environ. Res. Lett.*, in revision.
- Gutjahr, O., Putrasahan, D., Lohmann, K., Jungclaus, J. H., von Storch, J.-S., Brüggemann, N., Haak, H., Stössel, A. (2019).
 670 Max Planck Institute Earth System Model (MPI-ESM1.2) for the High-Resolution Model Intercomparison Project (HighResMIP), *Geosci. Model Dev.*, 12, 3241–3281, <https://doi.org/10.5194/gmd-12-3241-2019>.
- Gutowski Jr., W. J., Giorgi, F., Timbal, B., Frigon, A., Jacob, D., Kang, H.-S., Raghavan, K., Lee, B., Lennard, C., Nikulin, G., O'Rourke, E., Rixen, M., Solman, S., Stephenson, T., and Tangang, F. (2016). WCRP COordinated Regional
 675 Downscaling EXperiment (CORDEX): a diagnostic MIP for CMIP6, *Geosci. Model Dev.*, 9, 4087–4095, <https://doi.org/10.5194/gmd-9-4087-2016>.
- Haarsma, R. J., W. Hazeleger, C. Severijns, H. de Vries, A. Sterl, R. Bintanja, G. J. van Oldenborgh, H. W. van den Brink
 680 (2013). More hurricanes to hit Western Europe due to global warming. *Geophys. Res. Lett.*, 40, 1783–1788, doi:10.1002/grl.50360
- Haarsma, R. J., Roberts, M. J., Vidale, P. L., Senior, C. A., Bellucci, A., Bao, Q., Chang, P., Corti, S., Fučkar, N. S., Guemas, V., von Hardenberg, J., Hazeleger, W., Kodama, C., Koenigk, T., Leung, L. R., Lu, J., Luo, J.-J., Mao, J., Mizielinski, M. S., Mizuta, R., Nobre, P., Satoh, M., Scoccimarro, E., Semmler, T., Small, J., von Storch, J.-S. (2016). High



- 685 Resolution Model Intercomparison Project (HighResMIP v1.0) for CMIP6, *Geosci. Model Dev.*, 9, 4185–4208,
<https://doi.org/10.5194/gmd-9-4185-2016>.
- Haarsma, R., M. Acosta, R. Bakhshi, P.-A. Bretonnière, L.-P. Caron, M. Castrillo, S. Corti, P. Davini, E. Exarchou, F. Fabiano, U.
 690 Fladrich, R. Fuentes, J. García-Serrano, J. von Hardenberg, T. Koenigk, X. Levine, V. Meccia, T. van Noije, G. van den Oord, F.
 Palmeiro, M. Rodrigo, Y. Ruprich-Robert, P. Le Sager, E. Tourigny, S. Wang, M. van Weele, K. Wyser, (2019). HighResMIP
 versions of EC-Earth: EC-Earth3P and EC-Earth3P-HR. Description, model performance, data handling and validation.
Geosci. Model Dev., submitted.
- 695 Hall, A. (2014). Projecting regional change. *Science*, 346, 1460–1462. <https://doi.org/10.1126/science.aaa0629>
- Herrera, S., Gutiérrez, J. M., Ancell, R., Pons, M. R., Frías, M. D., Fernández, J. (2012). Development and analysis of a 50-
 year high-resolution daily gridded precipitation dataset over Spain (Spain02). *Int. J. Climatology*, 32, 74–85, doi:
 10.1002/joc.2256.
- 700 Hourdin, F., T. Mauritsen, A. Gettelman, J. Golaz, V. Balaji, Q. Duan, D. Folini, D. Ji, D. Klocke, Y. Qian, F. Rauser, C.
 Rio, L. Tomassini, M. Watanabe, D. Williamson (2017). The Art and Science of Climate Model Tuning. *Bull. Amer.*
Meteor. Soc., 98, 589–602, <https://doi.org/10.1175/BAMS-D-15-00135.1>
- 705 Iles, C. E., Vautard, R., Strachan, J., Joussaume, S., Eggen, B. R., and C. D. Hewitt (2019). The benefits of increasing
 resolution in global and regional climate simulations for European climate extremes, *Geoscientific Model Development*
Discussion, <https://doi.org/10.5194/gmd-2019-253>
- Isotta, F. A., C. Frei, V. Weigluni, M. P. Tadić, P. Lassègues, B. Rudolf, V. Pavan, C. Cacciamani, G. Antolini, S. M. Ratto,
 710 M. Munari, S. Micheletti, V. Bonati, C. Lussana, C. Ronchi, E. Panettieri, G. Marigo, G. Vertačnik (2014). The climate of
 daily precipitation in the Alps: development and analysis of a high-resolution grid dataset from pan-Alpine rain-gauge data.
Int. J. Climatol., 34, 1657–1675. doi: 10.1002/joc.3794
- Jacob, D., Petersen, J., Eggert, B. et al. (2014). EURO-CORDEX: new high-resolution climate change projections for
 715 European impact research. *Reg. Environ. Change*, 14, 563–578, doi: 10.1007/s10113-013-0499-2
- Jung, T., M. J. Miller, T. N. Palmer, P. Towers, N. Wedi, D. Achuthavarier, J. M. Adams, E. L. Altshuler, B. A. Cash, J. L.
 Kinter III, L. Marx, C. Stan, K. I. Hodges (2012). High-resolution global climate simulation with the ECMWF model in
 project Athena: Experimental design, model climate, and seasonal forecast skill. *J. Clim.*, 25, 3155–3172, doi: 10.1175/JCLI-
 D-11-00265.1
- 720 Jury, M. W., Herrera, S., Gutiérrez, J. M., Barriopedro, D. (2019). Blocking representation in the ERA-Interim driven
 EURO-CORDEX RCMs. *Clim. Dyn.*, 52, 3291–3306. <https://doi.org/10.1007/s00382-018-4335-8>
- 725 Kendon, E. J., Stratton, R. A., Tucker, S., Marsham, J. H., Berthou, S., Rowell, D. P., Senior, C. A. (2019). Enhanced future
 changes in wet and dry extremes over Africa at convection-permitting scale. *Nat. Commun.*, 10, 1794, doi:10.1038/s41467-
 019-09776-9
- Kerr, R. A. (2011). Vital details of global warming are eluding forecasters. *Science*, 334, 173–174.
- 730 Kerr, R. A. (2013). Forecasting regional climate change flunks its first test. *Science*, 339, 638.
- Kinter III, J. L., B. Cash, D. Achuthavarier, J. Adams, E. Altshuler, P. Dirmeyer, B. Doty, B. Huang, E. K. Jin, L. Marx, J.
 Manganello, C. Stan, T. Wakefield, T. Palmer, M. Hamrud, T. Jung, M. Miller, P. Towers, N. Wedi, M. Satoh, H. Tomita, C.
 Kodama, T. Nasuno, K. Oouchi, Y. Yamada, H. Taniguchi, P. Andrews, T. Baer, M. Ezell, C. Halloy, D. John, B. Loftis, R.



- 735 Mohr, K. Wong (2013). Revolutionizing Climate Modeling with Project Athena: A Multi-Institutional, International Collaboration. *Bull. Amer. Meteor. Soc.*, 94, 231–245.
- Kjellström E., Barring L., Nikulin G., Nilsson C., Persson G., Strandberg G. (2016). Production and use of regional climate model projections—A Swedish perspective on building climate services. *Clim. Serv.*, 2, 15–29.
- 740 Klingaman, N. P., Martin, G. M., and Moise, A. (2017). ASoP (v1.0): a set of methods for analyzing scales of precipitation in general circulation models. *Geoscientific Model Development*, 10(1), 57–83. <https://doi.org/10.5194/gmd-10-57-2017>
- 745 Kotlarski, S., Keuler, K., Christensen, O. B., Colette, A., Déqué, M., Gobiet, A., Goergen, K., Jacob, D., Lüthi, D., van Meijgaard, E., Nikulin, G., Schär, C., Teichmann, C., Vautard, R., Warrach-Sagi, K., Wulfmeyer, V. (2014). Regional climate modeling on European scales: a joint standard evaluation of the EURO-CORDEX RCM ensemble, *Geosci. Model Dev.*, 7, 1297–1333, <https://doi.org/10.5194/gmd-7-1297-2014>.
- 750 Kumar, D., Kodra, E., Ganguly, A. R. (2014). Regional and seasonal intercomparison of CMIP3 and CMIP5 climate model ensembles for temperature and precipitation. *Clim. Dyn.*, 43, 2491–2518. doi:10.1007/s00382-014-2070-3
- Lawrence, B. N., Bennett, V. L., Churchill, J., Juckes, M., Kershaw, P., Pascoe, S., Pepler, S., Pritchard, M. and Stephens, A. (2013). Storing and manipulating environmental big data with JASMIN. In: *IEEE Big Data*, October 6-9, 2013, San Francisco. <https://doi.org/10.1109/BigData.2013.6691556>.
- 755 Luu, L., R. Vautard, P. Yiou, G. J. van Oldenborgh, and G. Lenderink (2018). Attribution of extreme rainfall events in the South of France using EURO-CORDEX simulations. *Geophys. Res. Lett.*, doi :10.1029/2018GL077807
- 760 Matsueda, M. and T. N. Palmer (2011). Accuracy of climate change predictions using high resolution simulations as surrogates of truth. *Geophys. Res. Lett.*, 38, L05803.
- Mauritsen, T., Stevens, B., Roeckner, E., Crueger, T., Esch, M., Giorgetta, M., Haak, H., Jungclaus, J., Klocke, D., Matei, D., Mikolajewicz, U., Notz, D., Pincus, R., Schmidt, H., Tomassini L. (2012). Tuning the climate of a global model, *J. Adv. Model. Earth Syst.*, 4, M00A01, doi:10.1029/2012MS000154.
- 765 Minobe, S., A. Kuwano-Yoshida, N. Komori, S.-P. Xie, R. J. Small (2008). Influence of the Gulf Stream on the troposphere. *Nature*, 452, 206–209, doi:10.1038/nature06690
- 770 Perry, M., Hollis, D., Elms, M. (2009). The generation of daily gridded datasets of temperature and rainfall for the UK, Climate Memorandum No.24, National Climate Information Centre, Met Office, Exeter, UK. Available at: https://www.metoffice.gov.uk/binaries/content/assets/metofficegovuk/pdf/weather/learn-about/uk-past-events/papers/cm24_generation_of_daily_gridded_datasets.pdf
- 775 Prein A. F., Gobiet A., Suklitsch M., Truhetz H., Awan N. K., Keuler K., Georgievski G. (2013). Added value of convection permitting seasonal simulations. *Clim. Dyn.*, 41, 2655–2677. <https://doi.org/10.1007/s00382-013-1744-6>.
- Prein A. F., Langhans W., Fosse G., Ferrone A., Ban N., Goergen K., Keller M., Tölle M., Gutjahr O., Feser F., Brisson E., Kollet S., Schmidli J., Van Lipzig N. P. M., Leung R. (2015). A review on regional convection-permitting climate modeling: Demonstrations, prospects, and challenges. *Rev Geophys.* 53, 323–361. <https://doi.org/10.1002/2014RG000475>.
- 780 Prein, A. F., A. Gobiet, H. Truhetz, K. Keuler, K. Goergen, C. Teichmann, C. Fox Maule, E. van Meijgaard, M. Déqué, G. Nikulin, R. Vautard, A. Colette, E. Kjellström, D. Jacob (2016). Precipitation in the EURO-CORDEX 0.11° and 0.44° simulations: high resolution, high benefits? *Clim Dyn*, 46, 383–412. <https://doi.org/10.1007/s00382-015-2589-y>



- 785 Prein, A. F. and A. Gobiet (2017). Impacts of uncertainties in European gridded precipitation observations on regional climate analysis. *Int. J. Climatol.*, 37, 305–327, doi: 10.1002/joc.4706
- Rajczak, J. and Schär, C. (2017). Projections of future precipitation extremes over Europe: a multimodel assessment of climate simulations. *J. Geophys. Res. Atmos.*, 122, 10773–10800. <https://doi.org/10.1002/2017JD027176>
- 790 Randall, D. A., R. A. Wood, S. Bony, R. Colman, T. Fiechfet, J. Fyfe, V. Kattsov, A. Pitman, J. Shukla, J. Srinivasan, R. J. Stouffer, A. Sumi and K. E. Taylor (2007). *Climate Models and Their Evaluation*. In: *Climate Change 2007: The Physical Science Basis. Contribution of Working Group I to the Fourth Assessment Report of the Intergovernmental Panel on Climate Change* [Solomon, S., D. Qin, M. Manning, Z. Chen, M. Marquis, K. B. Averyt, M. Tignor and H. L. Miller (eds.)]. Cambridge University Press, Cambridge, United Kingdom and New York, NY, USA.
- 795 Roberts, C. D.; Senan, R.; Molteni, F.; Boussetta, S.; Keeley, S. (2017). ECMWF ECMWF-IFS-HR model output prepared for CMIP6 HighResMIP hist-1950. Version 20170915. Earth System Grid Federation. <https://doi.org/10.22033/ESGF/CMIP6.4981>
- 800 Roberts, C. D., Senan, R., Molteni, F., Boussetta, S., Mayer, M., and Keeley, S. P. E. (2018). Climate model configurations of the ECMWF Integrated Forecasting System (ECMWF-IFS cycle 43r1) for HighResMIP, *Geosci. Model Dev.*, 11, 3681–3712, <https://doi.org/10.5194/gmd-11-3681-2018>.
- 805 Roberts, M. J., P. L. Vidale, M. S. Mizieliński, M.-E. Demory, R. Schiemann, J. Strachan, K. Hodges, R. Bell, J. Camp (2015). Tropical Cyclones in the UPSCALE Ensemble of High-Resolution Global Climate Models. *J. Climate*, 28, 574–596, <https://doi.org/10.1175/JCLI-D-14-00131.1>
- 810 Roberts, M. J., H. T. Hewitt, P. Hyder, D. Ferreira, S. A. Josey, M. Mizieliński, and A. Shelly (2016). Impact of ocean resolution on coupled air-sea fluxes and large-scale climate. *Geophys. Res. Lett.*, 43, 10430–10438, <https://doi.org/10.1002/2016GL070559>.
- 815 Roberts, M. (2018). MOHC HadGEM3-GC31-HM model output prepared for CMIP6 HighResMIP hist-1950. Version 20180730. Earth System Grid Federation. <https://doi.org/10.22033/ESGF/CMIP6.6040>
- 820 Roberts, M. J., P. L. Vidale, C. Senior, H. T. Hewitt, C. Bates, S. Berthou, P. Chang, H. M. Christensen, S. Danilov, M.-E. Demory, S. M. Griffies, R. Haarsma, T. Jung, G. Martin, S. Minobe, T. Ringler, M. Satoh, R. Schiemann, E. Scoccimarro, G. Stephens, M. F. Wehner (2018). The Benefits of Global High Resolution for Climate Simulation: Process Understanding and the Enabling of Stakeholder Decisions at the Regional Scale. *Bull. Amer. Meteor. Soc.*, 99, 2341–2359, <https://doi.org/10.1175/BAMS-D-15-00320.1>
- 825 Roberts, M. J., Baker, A., Blockley, E. W., Calvert, D., Coward, A., Hewitt, H. T., Jackson, L. C., Kuhlbrodt, T., Mathiot, P., Roberts, C. D., Schiemann, R., Seddon, J., Vannière, B., and Vidale, P. L. (2019). Description of the resolution hierarchy of the global coupled HadGEM3-GC3.1 model as used in CMIP6 HighResMIP experiments, *Geosci. Model Dev.*, 12, 4999–5028, <https://doi.org/10.5194/gmd-12-4999-2019>.
- 830 Roberts, M. J., J. Camp, J. Seddon1, P. L. Vidale, K. Hodges, B. Vanniere, J. Mecking, R. Haarsma4, A. Bellucci, E. Scoccimarro, L.-P. Caron, F. Chauvin, L. Terray, S. Valcke, M.-P. Moine, D. Putrasahan, C. Roberts, R. Senan, C. Zarzycki, P. Ullrich. Impact of model resolution on tropical cyclone simulation using the HighResMIP-PRIMAVERA multi-model ensemble. *J. Clim.* (revised).
- Rummukainen, M. (2010). State-of-the-art with regional climate models. *WIREs Clim. Change*, 1, 82-96, doi:10.1002/wcc.8



- 835 Schär, C., O. Fuhrer, A. Arteaga, N. Ban, C. Charpillon, S. Di Girolamo, L. Hentgen, T. Hoefler, X. Lapillonne, D. Leutwyler, K. Osterried, D. Panosetti, S. Rüdisühli, L. Schlemmer, T. Schulthess, M. Sprenger, S. Ubbiali, H. Wernli (2019). Kilometer-scale climate models: Prospects and challenges. *Bull. American Meteorol. Soc.*, in press, <https://doi.org/10.1175/BAMS-D-18-0167.1>
- 840 Schiermeier, Q. (2010). The real holes in climate science. *Nature*, 463, 284–287.
- Scoccimarro, E., A. Bellucci, D. Peano (2018). CMCC CMCC-CM2-VHR4 model output prepared for CMIP6 HighResMIP hist-1950. Version 20180705. Earth System Grid Federation. <https://doi.org/10.22033/ESGF/CMIP6.3818>
- 845 Shaffrey, L. C., I. Stevens, W. A. Norton, M. J. Roberts, P. L. Vidale, J. D. Harle, A. Jrrar, D. P. Stevens, M. J. Woodage, M. E. Demory, J. Donners, D. B. Clark, A. Clayton, J. W. Cole, S. S. Wilson, W. M. Connolley, T. M. Davies, A. M. Iwi, T. C. Johns, J. C. King, A. L. New, J. M. Slingo, A. Slingo, L. Steenman-Clark, G. M. Martin (2009). U.K. HiGEM: the new U.K. High-Resolution Global Environment Model - Model description and basic evaluation. *J. Clim.*, 22, 1861–1896, doi: 10.1175/2008JCLI2508.1
- 850 Sørland, S. L., C. Schär, D. Lüthi, E. Kjellström (2018). Bias patterns and climate change signals in GCM-RCM model chains. *Environ. Res. Lett.*, 13, 074017. <https://doi.org/10.1088/1748-9326/aacc77>
- 855 Sørland, S., Knutti, R., Fischer, A., Kotlarski, S., Künsch, H.R., Liniger, M., Rajczak, J., Schär, C., Spirig, C., Strassmann, K., Zubler, E. CH2018 - New climate scenarios for Switzerland: How to construct multi-model projections from a complex model matrix. In preparation.
- Stephens, G. L., T. L'Ecuyer, R. Forbes, A. Gettleman, J.-C. Golaz, A. Bodas-Salcedo, K. Suzuki, P. Gabriel, J. Haynes (2010). Dreary state of precipitation in global models. *J. Geophys. Res.*, 115, D24211, doi: 10.1029/2010JD014532
- 860 Szalai, S., Auer, I., Hiebl, J., Milkovich, J., Radim, T., Stepanek, P., Zahradnicek, P., Bihari, Z., Lakatos, M., Szentimrey, T., Limanowka, D., Kilar, P., Cheval, S., Deak, Gy., Mihic, D., Antolovic, I., Mihajlovic, V., Nejedlik, P., Stastny, P., Mikulova, K., Nabyvanets, I., Skyryk, O., Krakovskaya, S., Vogt, J., Antofie, T., Spinoni, J.: Climate of the Greater Carpathian Region. Final Technical Report. www.carpatclim-eu.org.
- 865 Torma, C., F. Giorgi, E. Coppola (2015). Added value of regional climate modeling over areas characterized by complex terrain—Precipitation over the Alps, *J. Geophys. Res. Atmos.*, 120, 3957–3972, doi:10.1002/2014JD022781.
- 870 Vannière, B., Demory, M.-E., Vidale, P. L., Schiemann, R., Roberts, M. J., Roberts, C. D., Matsueda, M., Terray, L., Koenigk, T., Senan, R. (2019). Multi-model evaluation of the sensitivity of the global energy budget and hydrological cycle to resolution. *Clim. Dyn.*, 52, 6817–6846, doi:10.1007/s00382-018-4547-y
- Vautard, R., N. Kadyrov, C. Iles, F. Boberg, E. Buonomo, E. Coppola, K. Bülow, L. Corre, E. van Meijgaard, R. Nogherotto, et al. Assessment of the large EURO-CORDEX regional climate simulation ensemble. In preparation.
- 875 Vidal, J. P., Martin, E., Franchisteguy, L., Baillon, M., Soubeyroux, J.-M. (2010). A 50-year high-resolution atmospheric reanalysis over France with the Safran system. *Int. J. Climatol.*, 30, 1627–1644, doi: 10.1002/joc.2003.
- Voldoire, A. (2019). CNRM-CERFACS CNRM-CM6-1-HR model output prepared for CMIP6 HighResMIP hist-1950. Version 20190221. Earth System Grid Federation. <https://doi.org/10.22033/ESGF/CMIP6.4040>
- 880 Voldoire, A., Saint-Martin, D., Sénési, S., Decharme, B., Alias, A., Chevallier, M., et al. (2019). Evaluation of CMIP6 DECK experiments with CNRM-CM6-1. *Journal of Advances in Modeling Earth Systems*, 11, 2177–2213. <https://doi.org/10.1029/2019MS001683>



- 885 von Storch, J.-S.; Putrasahan, D.; Lohmann, K.; Gutjahr, O.; Jungclaus, J.; Bittner, M.; Haak, H.; Wieners, K.-H.; Giorgetta, M.; Reick, C.; Esch, M.; Gayler, V.; de Vrese, P.; Raddatz, T.; Mauritsen, T.; Behrens, J.; Brovkin, V.; Claussen, M.; Crueger, T.; Fast, I.; Fiedler, S.; Hagemann, S.; Hohenegger, C.; Jahns, T.; Kloster, S.; Kinne, S.; Lasslop, G.; Kornblueh, L.; Marotzke, J.; Matei, D.; Meraner, K.; Mikolajewicz, U.; Modali, K.; Müller, W.; Nabel, J.; Notz, D.; Peters, K.; Pincus, R.; Pohlmann, H.; Pongratz, J.; Rast, S.; Schmidt, H.; Schnur, R.; Schulzweida, U.; Six, K.; Stevens, B.; Voigt, A.;
- 890 Roeckner, E. (2018). MPI-M MPI-ESM1.2-XR model output prepared for CMIP6 HighResMIP hist-1950. Version 20180606. Earth System Grid Federation. <https://doi.org/10.22033/ESGF/CMIP6.10307>
- Woollings, T., Hannachi, A., Hoskins, B. (2010). Variability of the North Atlantic eddy-driven jet stream. Q.J.R. Meteorol. Soc., 136, 856-868, doi:10.1002/qj.625
- 895 Zhao, M., Held, I. M., Lin, S.-J., Vecchi, G. A. (2009). Simulations of Global Hurricane Climatology, Interannual Variability, and Response to Global Warming Using a 50-km Resolution GCM. J. Climate, 33, 6653-6678.

Model name	HadGEM3-GC31-HM	EC-Earth3P-HR	CNRM-CM6-1-HR	MPI-ESM1-2-XR	CMCC-CM2-VHR4	ECMWF-IFS-HR
Institute	Met Office	KNMI, SMHI, BSC, CNR	CERFACS	MPI-M	CMCC	ECMWF
Reference	Roberts et al., 2019	Haarsma et al., 2019	Voltaire et al., 2019	Gutjahr et al., 2019	Cherchi et al., 2019	Roberts et al., 2018
Atmosphere horizontal resolution (in km at 50N)	N512 (25km)	TI511 (36km)	TI359 (50km)	T255 (34km)	0.25° (18km)	Tco399 (25km, output at 50km)
Ocean resolution (km)	25km	25km	25km	40km	25km	25km
Simulation	hist-1950	hist-1950	hist-1950	hist-1950	hist-1950	hist-1950
Ensemble member	r1i1p1f1	r1i1p2f1	r1i1p1f2	r1i1p1f1	r1i1p1f1	r1i1p1f1

900 **Table 1: Information about the PRIMAVERA high-resolution GCMs used in this study, including their spatial resolution (for full details, refer to <https://www.primavera-h2020.eu/modelling/our-models/>). The ones listed in bold are of the same family than the CMIP5 GCMs downscaled by CORDEX.**

HighResMIP equiv.	CMIP5 GCMs	EUR-44 RCMs	EUR-11 RCMs
CNRM-CM6-1-HR	CNRM-CM5 r1	RCA4 ALADIN53 ALARO CCLM5	RCA4 ALADIN53 ALARO CCLM4 ALADIN63 RACMO22E HIRHAM5
EC-Earth3P-HR	EC-EARTH r1	RACMO22E WRF341E	RACMO22E HIRHAM5*
	EC-EARTH r3	HIRHAM5	HIRHAM5* RCA RACMO22E
	EC-EARTH r12	RCA4 CCLM5	RCA4 CCLM4 RACMO22E HIRHAM5
MPI-ESM1-2-XR	MPI-ESM-LR r1	RCA4 CCLM4 REMO09 CCLM5	RCA4 CCLM4 REMO09
	MPI-ESM-LR r2		REMO09
HadGEM3-GC31-HM	HadGEM2-ES r1	RCA4 RACMO22E CCLM5 RegCM4	RCA4 RACMO22E CCLM4 HIRHAM5*
	IPSL-CM5A-MR r1	RCA4 WRF331F	RCA4 WRF331F REMO09
	NorESM1-M r1	RCA4	RCA4 REMO09 RACMO22E HIRHAM5*
	GFDL-ESM2M r1	RCA4	REMO09
	MIROC5 r1	RCA4 CCLM5	



905 **Table 2: Summary of historical EURO-CORDEX simulations used in this study. The first column indicates HighResMIP models of the same family as the CMIP5 GCM (second column) driving the RCMs. Matching colors show comparable HighResMIP GCMs and EURO-CORDEX RCMs. Within EURO-CORDEX RCMs, dark shaded models are available at both 0.11° (EUR-11) and 0.44 (EUR-44) horizontal resolutions. HIRHAM5* indicates several versions of this model were used. See Table S1 for the full list of EURO-CORDEX data used, including institutions and detailed RCM model version.**

Observations	SAFRAN	UKCPobs	CARPATCLIM	SPAIN02 v2 + PT02 v2	ALPS-EURO4M	E-OBS v17
Domain covered	France	British Isles	Carpathians	Iberian Peninsula	Alps	Other European regions
Spatial resolution	8km	5km	0.1°	0.2°	5km	0.5°
Temporal resolution	daily	daily	daily	daily	daily	daily
Time period considered	1971-2005	1971-2005	1971-2005	1971-2003	1971-2005	1971-2005

910 **Table 3: Information about the observational datasets used in this study (refer to Fig S1 for the coverage). The time period concerns that considered in this study, not the available period of each observational datasets.**

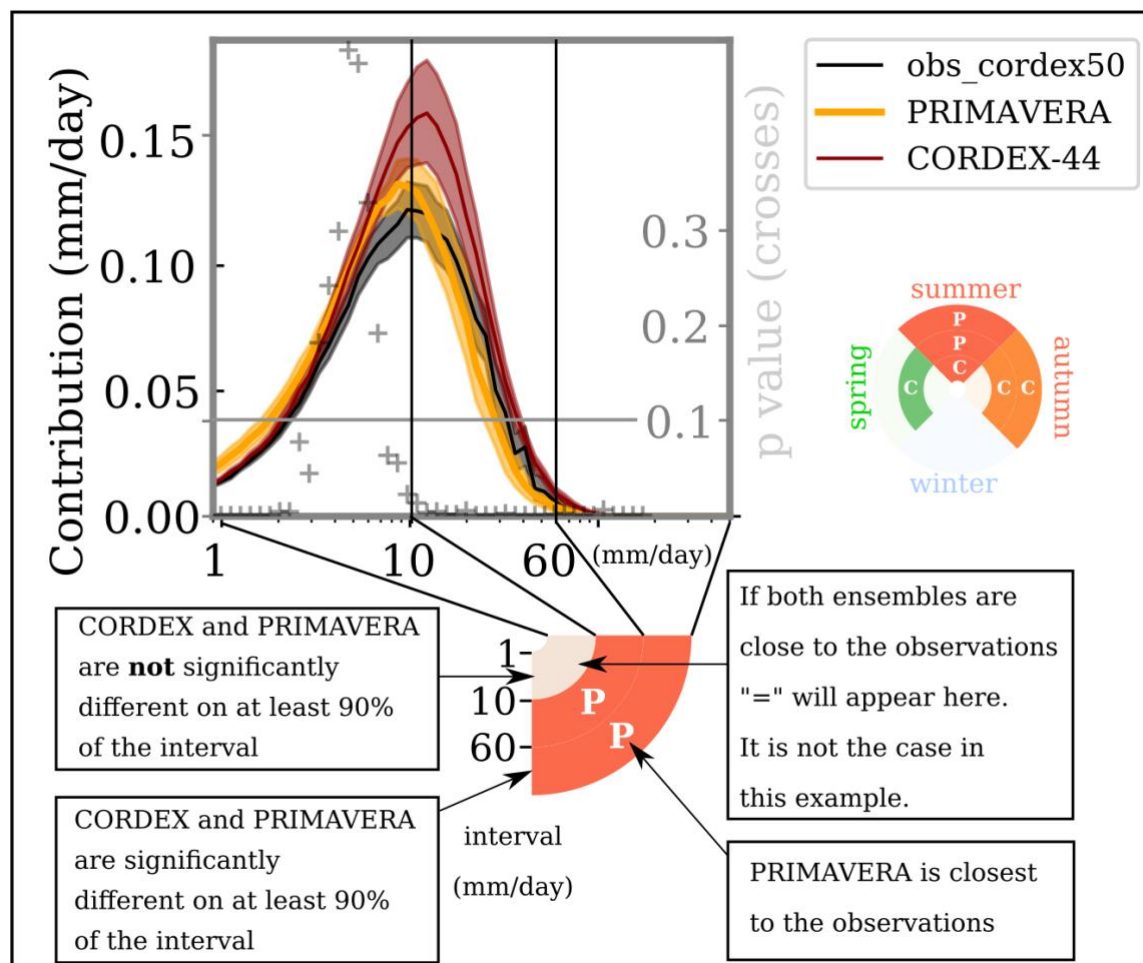
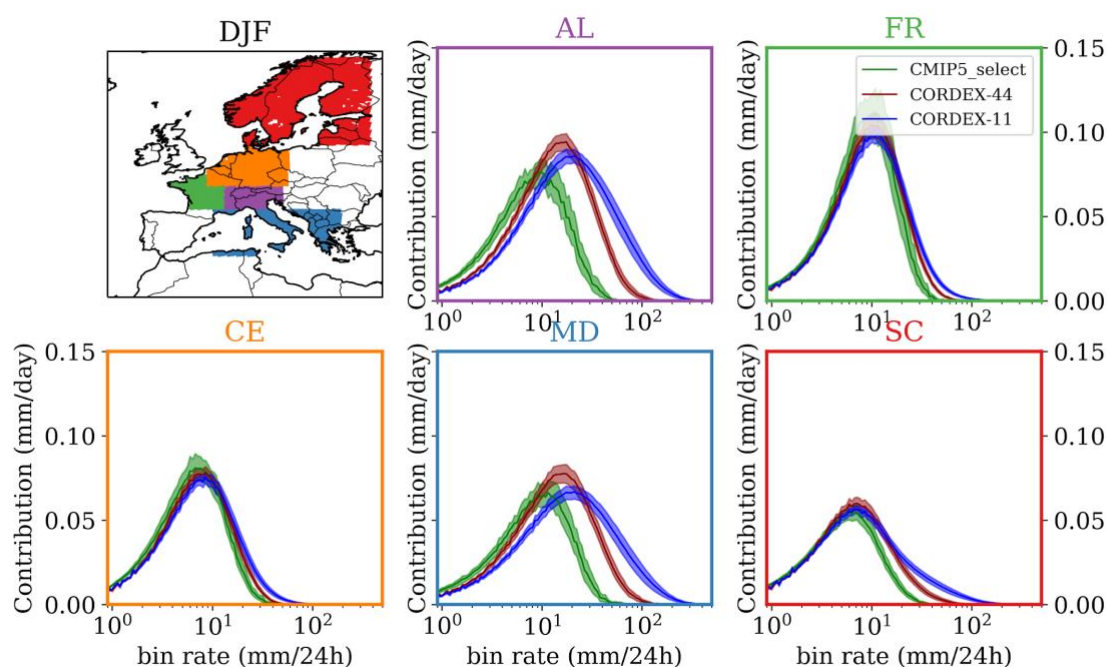


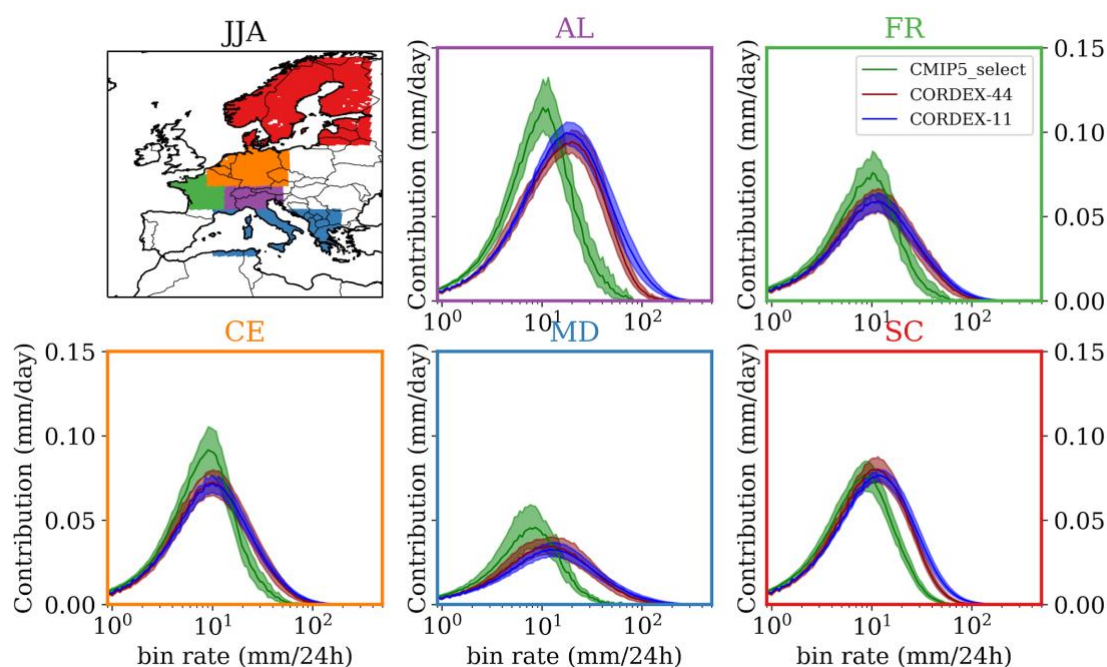
Figure 1: Explanation of the method: a) Daily precipitation contribution to the mean (precipitation frequency x bin intensity), with exponential bins for the UK in summer (JJA) for the PRIMAVERA ensemble, the EUR-44 ensemble and the observations. Inter-member spread is shown for the models, inter-annual spread is shown for the observations. Grey crosses are the p -value of the PRIMAVERA vs CORDEX difference using a 1000 times bootstrap resampling (see text), the ensembles are significantly different where the crosses are below 0.1. For three precipitation intensity intervals (low: 1-10, middle: 10-60, high: >60 mm/day): if the ensembles differ on more than 90% of the interval, the pie chart (below the graph) is coloured. Letters show which ensemble is closest to the observations in that case. b) For each region, a pie chart is produced with the four seasons (DJF, MAM, JJA, SON) and the low, middle, high precipitation intensity intervals.

915



920

Figure 2: Precipitation contribution (frequency x bin rate) per rain rate in DJF over the Alps (AL), France (FR), Central Europe (CE), Mediterranean (MD), Scandinavian (SC) for a selection of CMIP5 GCMs (green), EUR-44 (red), EUR-11 (blue). All data are plotted on the models native grid.



925 **Figure 3: Similar to Fig. 2 for JJA.**

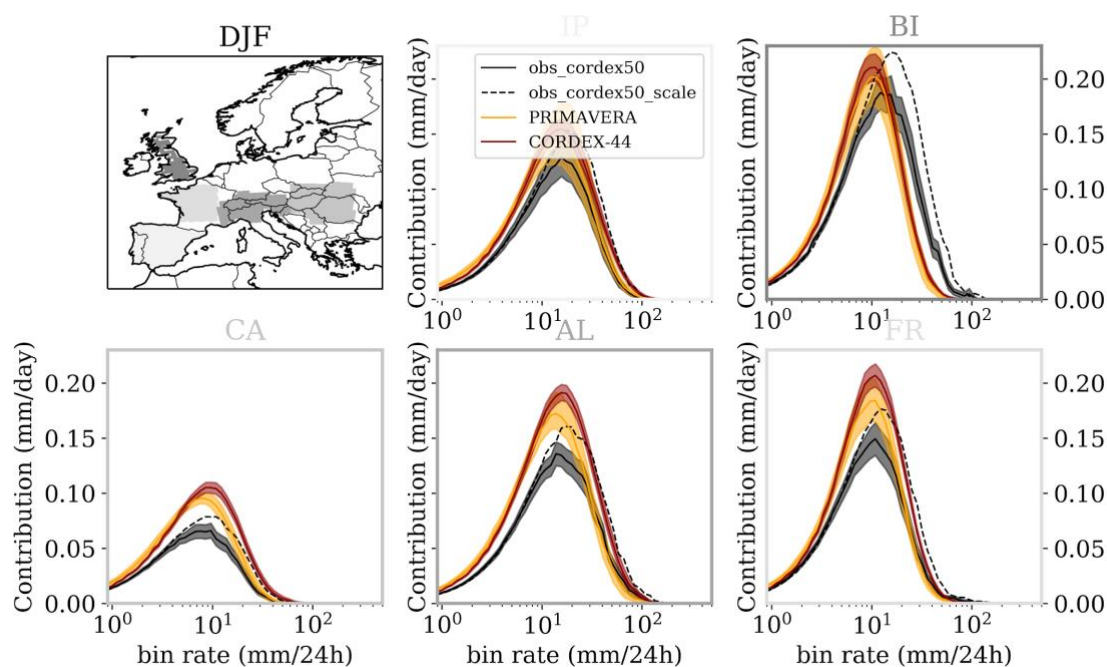


Figure 4: Precipitation contribution (frequency x bin rate) per rain rate in DJF over the Iberian Peninsula (IP), British Isles (BI), Carpathians (CA), Alps (AL), France (FR) for EUR-44 (red), PRIMAVERA (orange), observations regridded on EUR-44 (black) and a synthetic observational dataset taking into account an additional 20% undercatch error (dashed line).

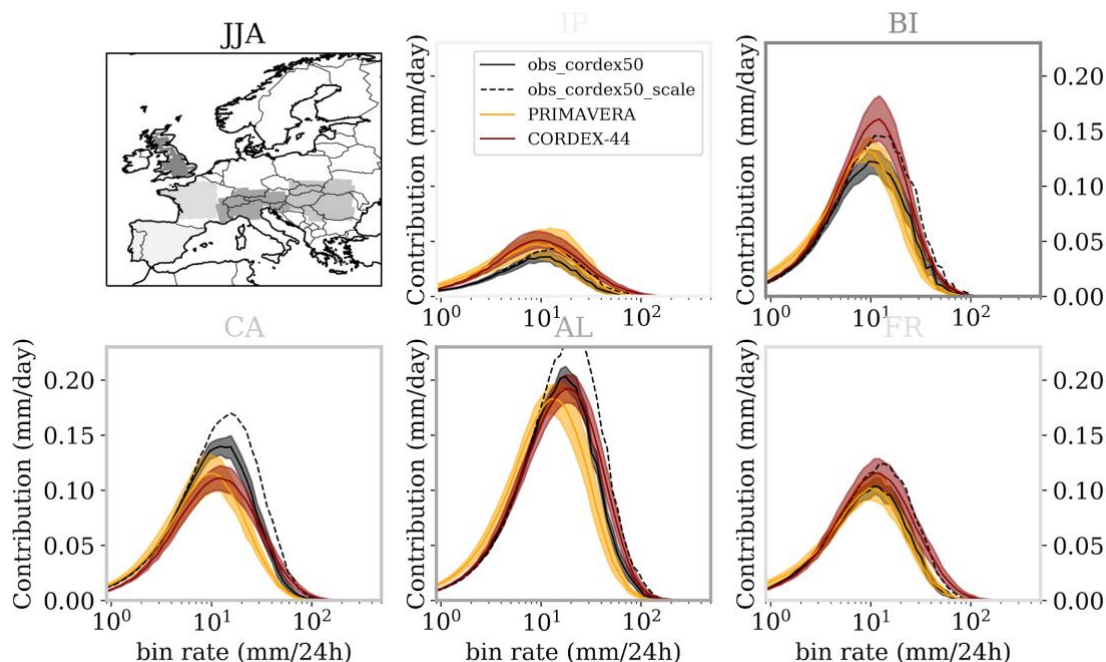


Figure 5: Same as Fig 4 for JJA.

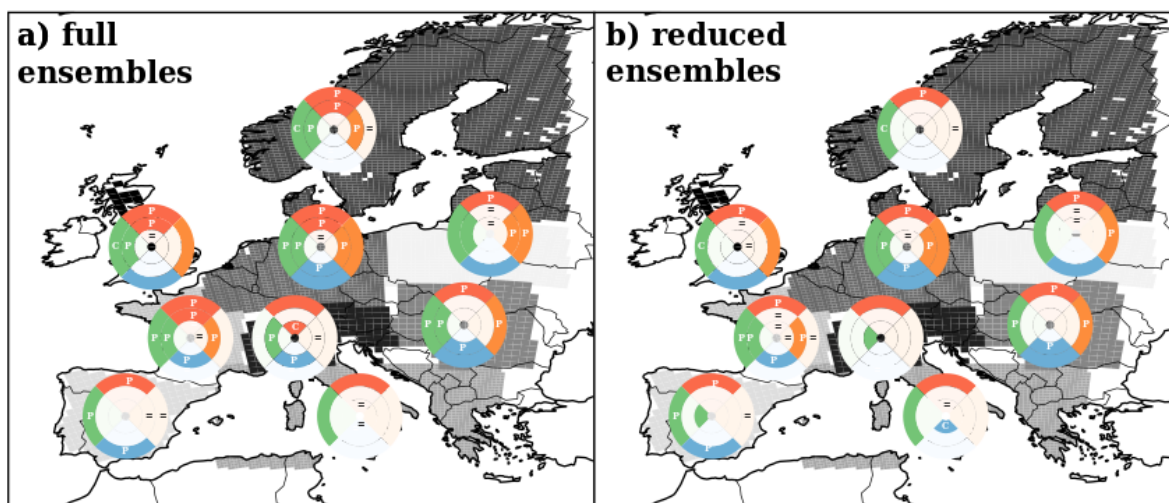
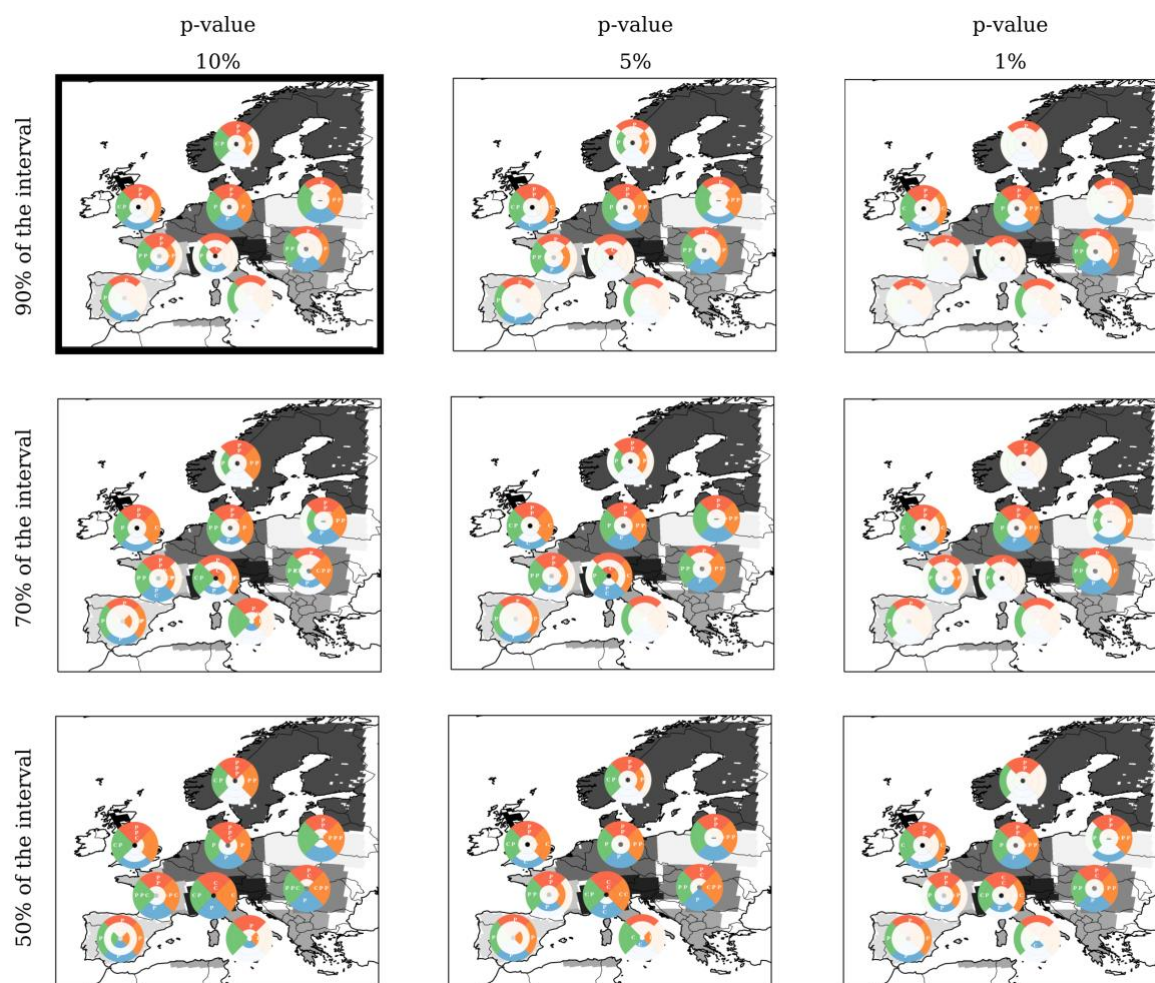


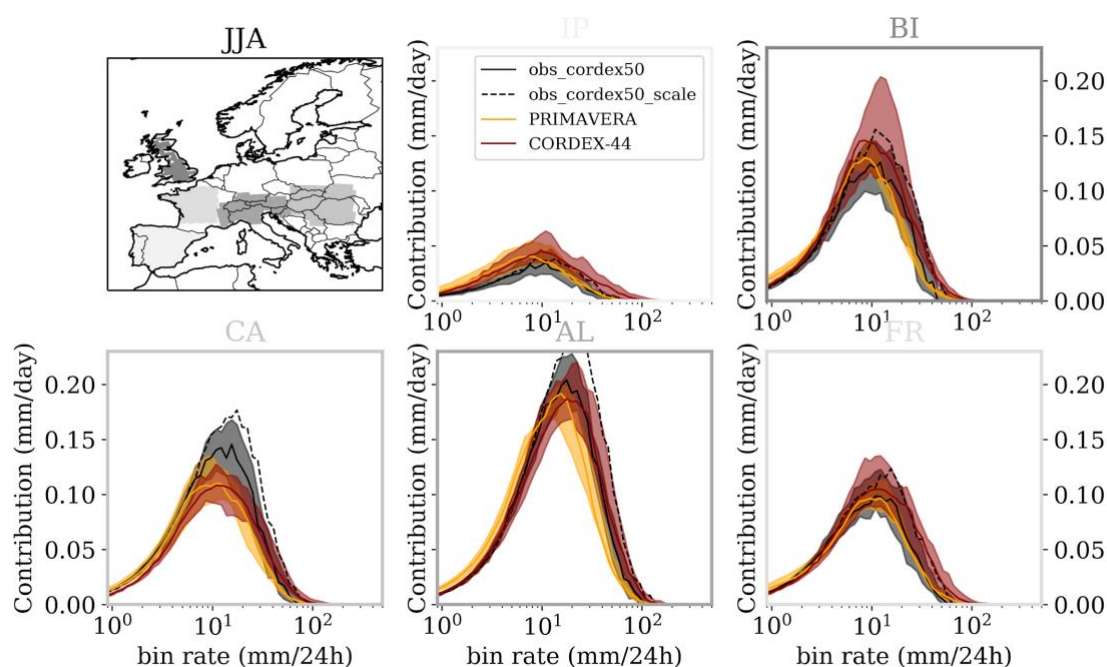
Figure 6: Map using the method described in Fig. 1: for each season (clockwise from the top: summer, autumn, winter, spring, see right panel of Fig. 1), region, and precipitation intensity interval (low rain rates=inner part, mid rain rates=middle part, high rain rates=outer part), a colour indicates that the CORDEX and PRIMAVERA ensembles are significantly different, a “P” or “C” letter indicates that PRIMAVERA or EUR-44 are closer to the observations, respectively, an “=” sign indicates that both ensembles



are close to observations. a) Map for the full PRIMAVERA and EUR-44 ensembles (listed in Tables 1 and 2); b) Map with reduced PRIMAVERA and EUR-44 ensembles using GCMs of the same family (coloured in Tables 1 and 2).



940 **Figure 7: Sensitivity of the pie charts to the significance thresholds used to determine 1) whether individual precipitation bins are significantly different between the two ensembles (left to right: 10, 5 or 1%) and 2) on which percentage of the precipitation interval the bins are different (bottom to top: 50, 70 or 90%). The bold frame shows the thresholds used in this study (Fig. 6).**



945 **Figure 8: Same as Fig. 5 with an interquartile range instead of bootstrap resampling 10% range. The thick lines show the model ensembles median, the shaded colours show the ensemble spread based on an interquartile (25th-75th percentile) method.**

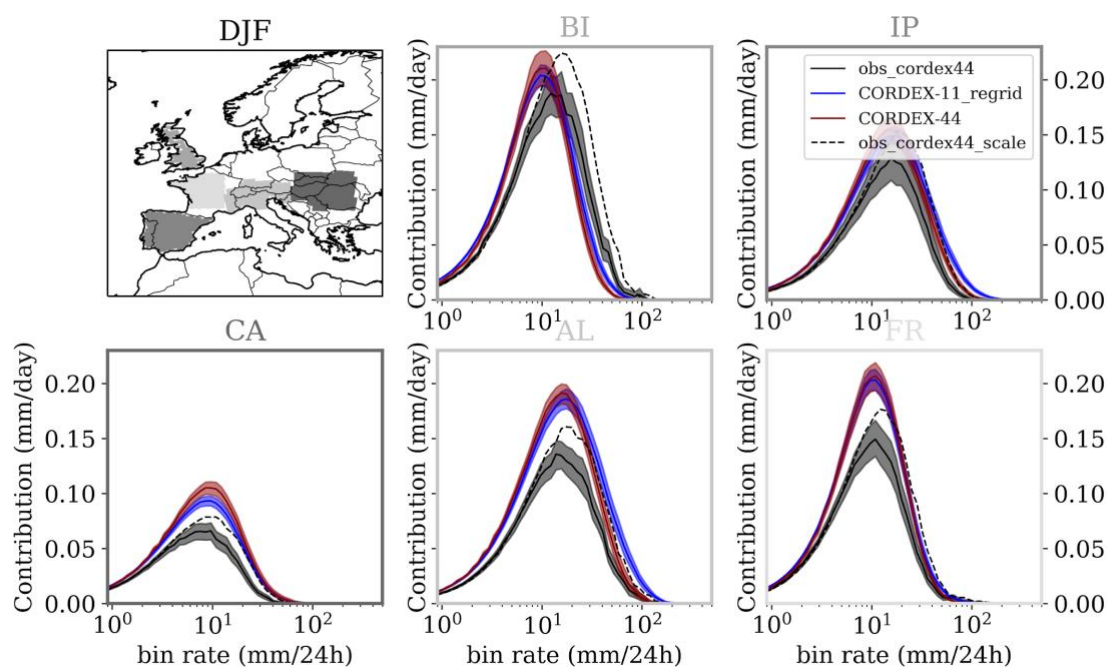




Figure 9: Precipitation contribution (frequency x bin rate) per rain rate in DJF over the Alps (AL), British Isles (BI), Iberian Peninsula (IP), Carpathians (CA) for EUR-44 (red), EUR-11 (blue) and observations (black). All data are computed on the EUR-44 grid.

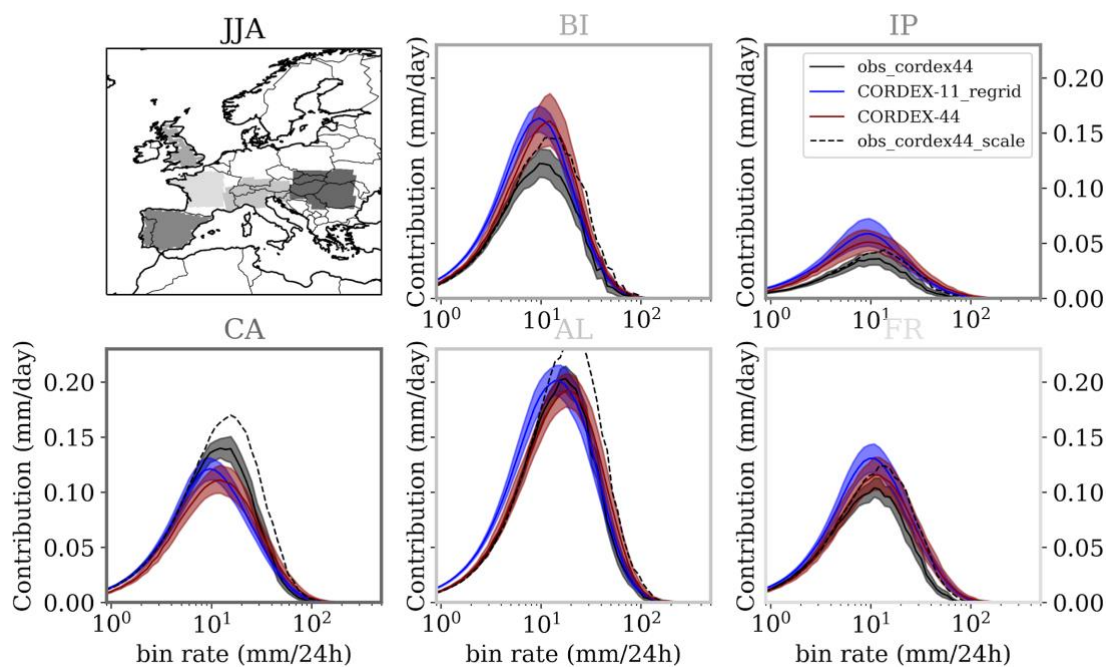


Figure 10: Same as Fig 9 for JJA.